A Georeferenced Digital Image Analysis of Micro-topographic Patterns within the Willamette Floodplain Research Natural Area, W.L. Finley National Wildlife Refuge

by

Karen L. Anderson

A Research Paper

submitted to

The Department of Geosciences
Oregon State University

in partial fulfillment of the requirements for the degree of

Master of Science
Geography Program

February 1996

directed by

Dr. Philip L. Jackson

ABSTRACT

The present day vegetation pattern of the Willamette Valley is a result of a long past of human alteration of the landscape. Beginning with aboriginal burning of the grasslands to present day land uses, the vegetation of the valley has been affected by anthropogenic activity. Wet prairie is a vanishing habitat of the valley as both urban and agricultural development continue to alter the landscape.

The W.L. Finley National Wildlife Refuge of the south-central Willamette Valley contains within its boundaries one of the last remaining examples of open wet prairie. In order to maintain the prairie community complex and associated biodiversity of the Willamette Valley Floodplain Research Natural Area, a restoration project in which controlled burning plays a significant role was initiated. As a part of the on-going research a need was felt to develop a baseline data base identifying the spatial distribution of principle features of the research area and to map the vegetationally associated mount-intermound micro-topographic pattern prevalent throughout the refuge.

The purpose of this research project was to develop that baseline spatial data base and to investigate the use of digital image processing and analysis as a tool for inventorying micro-topographic features and associated open wet prairie vegetation patterns. This paper is primarily a methodological study of applying geographic techniques to an on-going biogeographical study

This study had three objectives: (1) defining the location and boundaries of treatment spaces and sampling plots in a standard geographic coordinate system, (2) delineation of spaces and plots onto a scanned image creating a spatial data base and

(3) classification of vegetation and associated microtopography. The aim of this study is to provide an evaluation of appropriate geographic information technology for the planning and analysis of wetland restoration and management.

The objectives of this study were met with varying degrees of success. The use of Trimble's Global Positioning System, IDRISI's low-cost image processing/ Geographic Information System software and a small scale, color aerial photograph scanned to a single band, monochromatic digital image were utilized to create a suitable visual and spatial data base.

Classification of the image into micro-topographic class was conducted using three strategies. Two standard supervised classification algorithms were compared using signatures generated from the original single band image. The influence of including signatures created from an additional data band based on digital richness of the original image was also examined.

Information provided by the single, wide spectral space image was lacking and hampered classification of vegetationally associated micro-topographic patterns. The addition of signatures based on a created Relative Richness band did not appreciably effect classification accuracies. Regardless of classification strategy, insufficient separability of class signatures led to overall classification accuracies of +/- 70%. A high level of misclassification occurred within the intermound region resulting in over-representation of the mound micro-topographic pattern.

The resulting thematic map was created using signatures generated from the original single band image and maximum likelihood classification routine.

TABLE OF CONTENTS

LIST OF FIGURES

LIST OF TABLES

LIST OF APPENDICES

INTRODUCTION

The present day vegetation pattern of Oregon's Willamette Valley reflects a history of human manipulation of the natural landscape. Annual burning of prairies by Native Americans, cessation of burning with settlement and the introduction of grazing, logging and agriculture together with the continued expansion of agricultural clearance, alteration of natural drainage patterns, and urbanization profoundly influenced the vegetation composition and structure found in the Willamette Valley.

Today, the Willamette Floodplain Research Natural Area in W.L. Finley National Wildlife Refuge protects what is thought to be one of the few remaining examples of relatively unaltered open wet prairie. In the absence of fire and/or grazing the prairie would revert to forest. In order to restore and maintain the disclimax prairie in a condition similar to that at the time of settlement, a rigorous prescribed burning program was initiated in the Research Natural Area in 1990.

It is the purpose of this research paper to investigate the use of digital image analysis as a tool for inventorying micro-topographic features and associated open wet prairie vegetation patterns. The aim of this study is to provide an evaluation of appropriate geographic information technology for the planning and analysis of wetland restoration and management.

Objectives

As a part of the controlled burning program, long term research is being conducted to assess and document the topographic and ecological conditions of the Willamette Floodplain Research Natural Area (RNA). The objective of this study was to use digital image processing and classification techniques to develop a baseline geographic data base that would:

(1) map the boundaries of the RNA and research burn units,

(2) map the spatial distribution of permanent vegetation sampling plots within the RNA, and

(3) map the vegetationally associated mound-intermound micro-topographic pattern of the RNA.

To accomplish these objectives, I gathered spatial data using Global Positioning System (GPS) technology, mapped the spatial data with a computerized Geographic Information System (GIS) and identified and mapped the pattern of the vegetationally associated mound-intermound micro-topography. Mapping of the micro-topographic patterns was conducted using supervised classification techniques with available digital image processing and GIS software.

Historical Background

The north-south oriented Willamette Valley, approximately 130 miles long and 25-30 miles wide, is a physiographic region of western Oregon bounded on the east by the Cascade Range and the west by the Coast Range. Topography is predominantly flat, with slightly more relief to the north. Flowing northward, the Willamette River and its numerous tributaries form the drainage network for the region, eventually emptying into the Pacific-bound Columbia River north of Portland Oregon.

The valley has a mild climate. Annual temperatures range from highs of 18 degrees centigrade in July and August to lows of 3 degrees centigrade in January. Although precipitation occasionally occurs in summer, it is concentrated in late fall and winter from October through March with annual averages of approximately 890-1140 mm (Boyd 1986, 65). Low-intensity rains occur in the valley an average of 16-18 days during both December and January with the highest monthly precipitation of approximately 150-230 mm. during December (Jackson and Kimerling 1993, 53). Snow during the winter months is not

uncommon, yet usually moderate in amount, persisting on the ground for a matter of days. The mild climate, flat terrain and fertile alluvial soils attracted the first settlers arriving via the Oregon trail and led the valley to become a prime agricultural region of Oregon. The valley continues to be both the agricultural and population center of the state.

The semi-natural plant communities that today make up the Willamette Valley are reflective of past anthropogenic manipulation of the natural landscape. A meagerly documented prehistory of valley burning, a more recent and better documented history of agriculture and grazing with the advent of Euro-American settlement, and continued expansion of agricultural conversion and urban growth have all had a hand in altering the valley landscape and vegetation patterns.

Several authors have attempted to reconstruct, describe and map the original vegetation of the Willamette Valley (Habeck 1961, Johannessen et al. 1971, Towle 1979). Focusing on the period immediately prior to European settlement, researchers have reviewed early settler's journals, diaries, correspondences and environmental descriptions contained in the original General Land Office survey reports to reconstruct valley vegetation patterns. Although no direct evidence for the rational and procedures of Kalapuya burning exist, Boyd (1986) attempted to reconstruct both the practice and effect of purposeful burning upon the prairie while examining the interaction of the Kalapuya cultural ecology within the ecological context of the Willamette Valley. Prior to European settlement, the Kalapuya tribes were sole claimants to the territory of the mid-Willamette Valley. As hunter-gatherers, the Kalapuya were dependent upon the availability of wild game and wild plants for their livelihood. Annual settlement patterns of the Kalapuya revolved around the exploitation of valley resources.

The bulb of common camas (*Camassia quamash*) is often referred to as a dominant staple in the Kalapuya diet. Other important wild food plants include tarweed (*Madia* spp.),

hazel nuts(*Corylus*), acorns (*Quercus*), wapato (*Sagittaria*), and berries (Boyd 1986, 69). Gunther's ethnobotanical research of 18 tribes of western Washington describes numerous plant species important to the indigenous Native American lifestyle (Gunther 1973). Of those plant species listed by Gunther as being important sources of food and medicine or having uses as charms or textiles, sixteen are found within the prairie communities of the RNA (Appendix 1). In reviewing plants important in the Kalapuya diet, Towle (1971) notes that "it is clear that most of the plants eaten by the Kalapuya--including the staple camas--were dependent on maintenance of an open landscape" (Towle 1971, 18).

The importance of plant resources to the Kalapuya diet has been documented in archeological research. In their study of the dental pathology of Oregon's prehistoric indigenous population, Hall *et al.* (1986) examined dentitions of 208 prehistoric skeletal specimens from five geoclimatic-cultural regions of Oregon. Geoclimatic provinces were used to categorize heterogeneous cultural areas based on similarity of resource availability and utilization within the units. Of the five provinces studied, the Willamette Valley ranked second to the Klamath Basin in overall lowest dental status, ranking highest in incidences of caries (tooth decay) and edentulous jaws (0-2 teeth present at time of death) and second in pathologically missing teeth. As noted by Hall *et al.*, higher levels of caries and lower attrition are associated with a diet based predominately on plant resources and softer foods as was the case for the populations of the Willamette Valley and Klamath Basin (Hall *et al.* 1986).

The practice of annually burning the prairies to maximize resource production altered the ecology of the valley and maintained the productive expanses of disclimax grasslands and savanna. Euro-American settlers brought into the valley new expectations of the environment. Although the first settlers claimed land fringing the valley along the lower edges of the foothills (Boag 1992, 50), their impact was soon felt throughout the valley floor. The cessation of

purposeful burning as agriculture, and especially grazing, became predominant prairie activities led to significant historical changes in the valley landscape. As noted by Johannessen *et al.* (1971) the development of prairie and open woodland vegetation in the valley had probably been influence by fire for millennia (Johannessen et al. 1971, 292).

Today, the valley floor is dominated by agricultural lands and urban development. In the remaining open areas, cessation of fire has allowed succession to take place. The once open, fire resistant oak savanna and open grassland have become thickets of woody vegetation, dense woodlands, and maturing forest. Douglas-fir has become dominant in many areas over topping and inhibiting oak growth (Johannessen et al. 1971, 286). Remaining semi-natural communities include: oak woodlands, coniferous forests, riparian deciduous ash woodlands and forest and grasslands.

STUDY SITE

General Setting and Environment

The W.L. Finley National Wildlife Refuge, located approximately 20 km. south of Corvallis, west of U.S. Highway 99W (Figure 1), encompasses what is thought to be one on the few remaining examples of undisturbed open wet prairie. The United States Fish and Wildlife Service established the Willamette Floodplain Research Natural Area (RNA) within the refuge on December 27, 1966 to "...exemplify unplowed, near-natural grasslands" (Franklin *et al.* 1972). Enlarged in 1987, the Research Natural Area now consists of 200 hectares of open wet prairie.

A micro-topographic pattern of slightly raised, 40-50 cm., lenticular mounds surrounded by low-lying intermounds is the most striking topographic feature of the study site, distinguishable both in the field by vegetation structure and on low altitude aerial photographs by the distinctive patterning of topographically associated vegetation. This mound-intermound pattern is perhaps a remnant of past drainage patterns of the area (Frenkel and Streatfeild 1993, 2). While it has been claimed that the area had not *been plowed* or used for intensive agriculture (Franklin et al., 1972 and Moir and Mika, 1972), it had been heavily grazed by cattle (Frenkel and Streatfeild, 1994,1). It has been suggested that the higher elevated mound areas may have been shallow tilled and seeded at one time (Streatfeild-Welch 1995). Surrounded by agriculture, the RNA prairie drainage has been modified as indicated by several shallow ditches. Regionally available alien seeds have found their way into the RNA resulting in a highly altered floristic composition. Elimination of grazing in 1963, along with the cessation of purposeful burning, has allowed woody species such as rose (*Rosa* spp.), spirea (*Spirea douglasii*), hawthorn (*Crataegus douglasii*) and ash (*Fraxinus latifolia*) to invade the prairie RNA.

Willamette Floodplain Research Natural Area

W.L. Finley National Wildlife Refuge

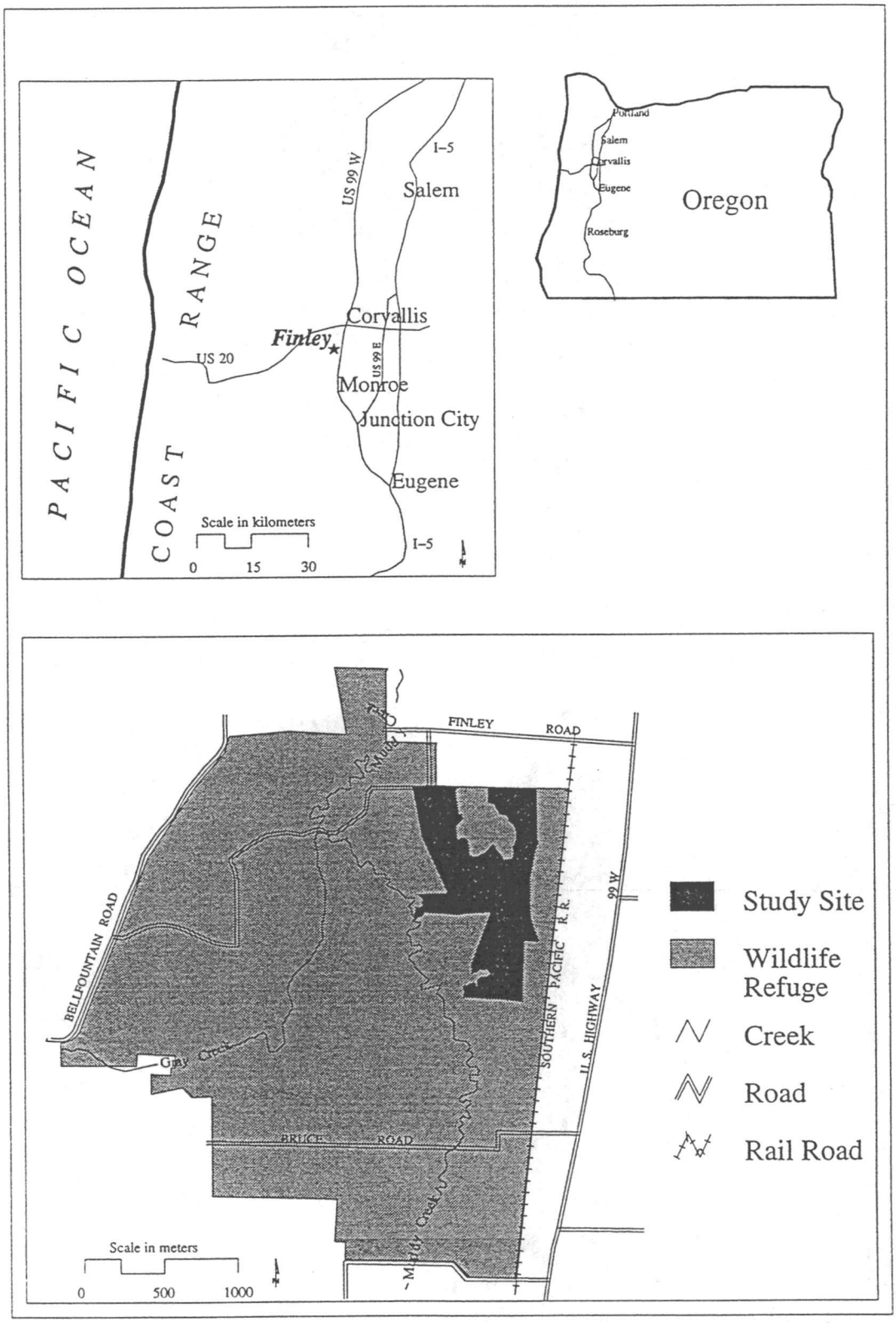

Figure 1. Location of the Willamette Floodplain Research Natural Area, W.L. Finley National Wildlife Refuge in reference to the Willamette Valley, OR.

At the time the RNA was established, Finley refuge staff realized that prescribed burning was necessary to restore and maintain the open prairie complex. Lack of a clear management plan and of a consistent burning program along with insufficient funding resulted in an haphazard burn history (Figure 2) with only limited post-burn ecological assessment having been conducted. Beginning in 1990 a prescribed burning management program, which included restoration research, was initiated and incorporated into the RNA management program. The overall purpose of the program was to restore the prairie, increase biodiversity and maintain a diversity of habitat and native species.

Concurrent RNA Ecological Research

The prescribed burning research program within the RNA addressed four primary concerns (Frenkel and Streatfeild 1994):

(1) consistent long term monitoring of vegetation and its response to fire,
(2) an effective long term burning program that maintains prairie vegetation,
(3) an accurate description of the present vegetation and its relation to environment, and
(4) an inventory of sensitive plant species.

Specific goals of this restoration research were to assess "the role of annual and triennial burning frequency on prairie composition and structure on mound and intermound topography" (Frenkel and Streatfeild 1993, 1).

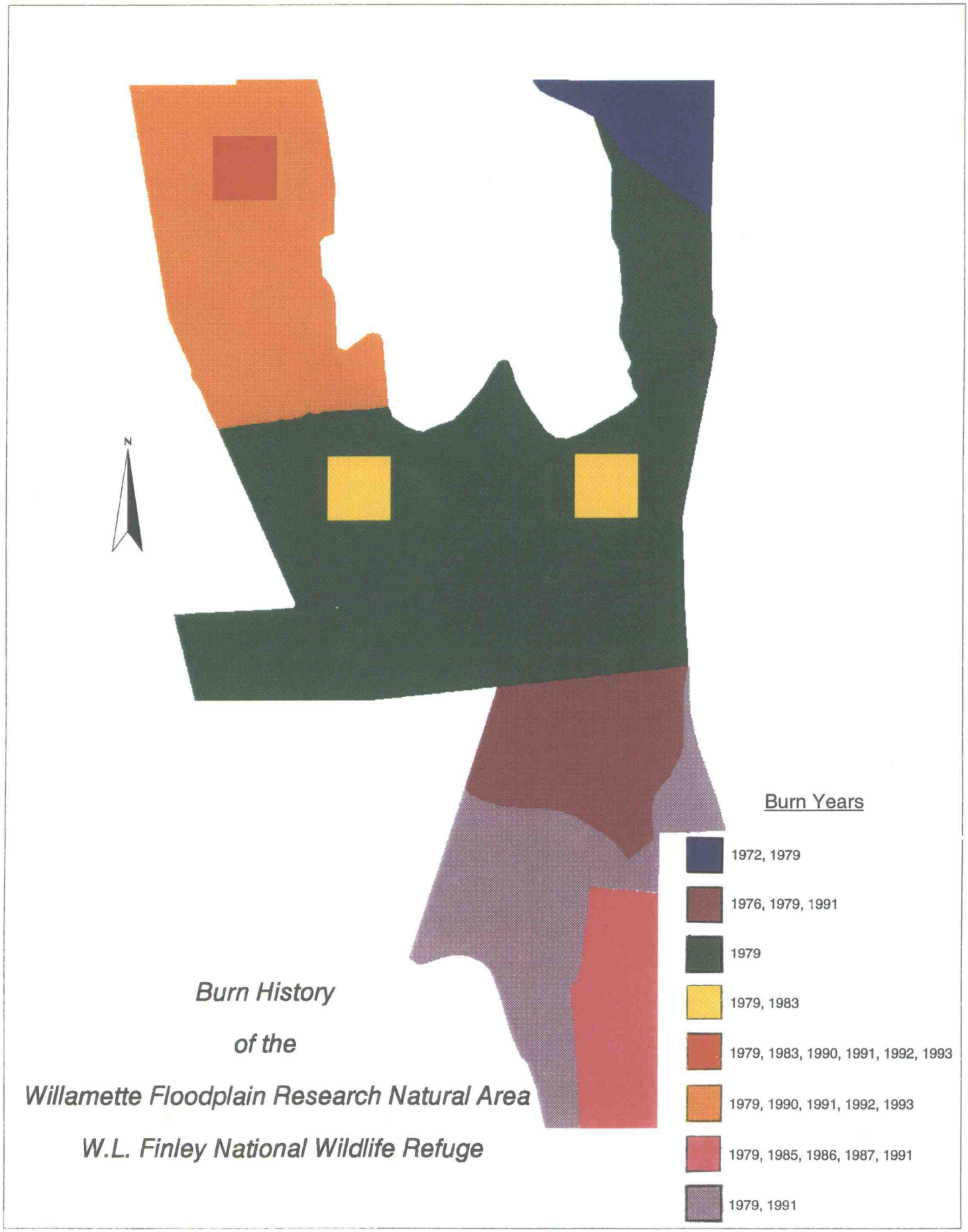

Figure 2. Burn history of research units within the Willamette Floodplain Research Natural Area, 1994.

To assess the impacts of prescribed burning upon plant communities associated with this micro-topographic pattern, the RNA was subdivided into four research "spaces" or burn treatment units with a planned burning schedule as follows:

Space 1: Burned annually beginning in 1990.

Space 2: Control area not to be burned.

Space 3: Burned triennially beginning in 1991.

Space 4: Burned triennially beginning in 1991 but with a complex prior burning history.

(Note that in 1979 an accidental fire swept through the entire area; thus, all spaces have a baseline burn history beginning in that year.)

In 1991 permanent vegetation sampling plots were established in the RNA by Streatfeild-Welch (1995). Delineation of the four treatment areas (Spaces 1-4) and the lenticular mound/intermound topographic pattern provided eight main sampling strata. Thirty-eight, 25 meter square vegetation plots (plots 1-36, 5a and 18a) were randomly selected from the strata such that at least 10 plots were selected each from Spaces 1-3 and six within smaller Space 4; they were equally distributed between mound and intermound topographic types (Figure 3). One-inch steel fence posts permanently mark the northwest and southwest corners of the plots.

Vegetation within permanent plots has been sampled annually since 1991 during late spring and early summer. Burn treatments have taken place in early fall. Using a one meter square nested frequency sampling frame, 25 random vegetation samples which include species identification, nested frequency and cover estimates have been collected within each plot (see Streatfeild-Welch (1995) for details on sampling design). Vegetation analysis was conducted by Frenkel with the use of the two-way indicator species analysis (TWINSPAN) statistical program for vegetation classification and non-metric multi-dimensional scaling (NMS)

Willamette Floodplain Research Natural Area

Research Spaces and Permanent Vegetation Sampling Plots

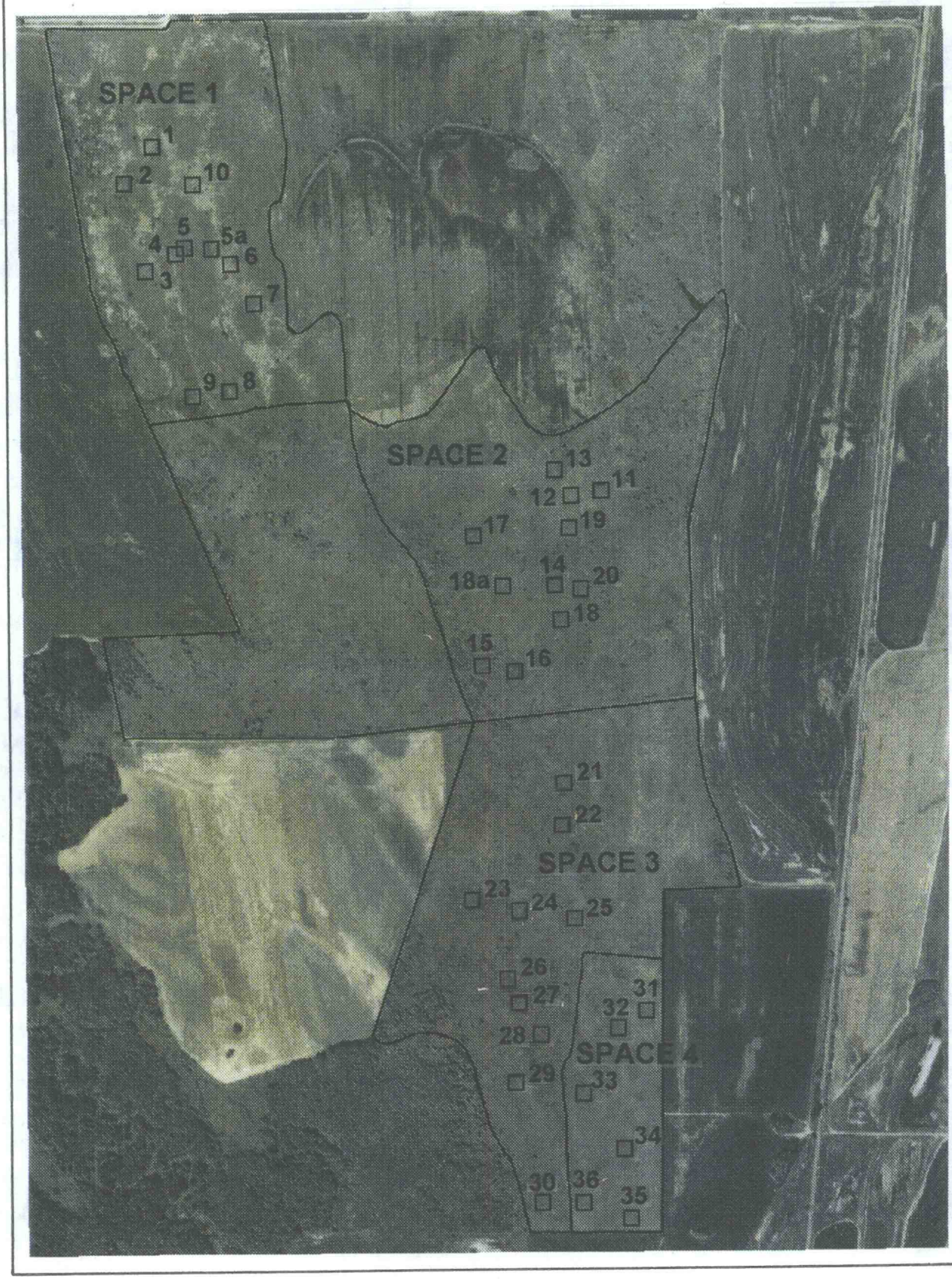

Figure 3. Delineation of research units and spatial distribution of permanent vegetation sampling plots.

ordination of the first year's data to investigate major environmental factors such as topography and moisture (Frenkel and Streatfeild 1994).

General characteristics of the mound-intermound topography are apparent in the field and observable on aerial photographs. They have been further investigated by Streatfeild-Welch (1995) using elevation transects along with vegetation sampling and analysis. Grasses, forbs and shrubs dominate the prairie landscape. Immature hawthorn (*Crataegus douglasii*) and *ash (Fraxinus latifolia*) can be found in scattered groups. Frenkel and Streatfeild (1994) found that the shrub and herb species are distributed with respect to topographic differences and that fire alters the makeup of these communities.

The raised, lenticular mounds are generally dominated by species associated with drier conditions. Shrub species such as *Rosa eglanteria* are more important in the mound rather than intermound habitats. Annuals account for 57.0% of the species found in mound communities. Introduced and native species are found in approximately equal proportions. Key mound species include: *Poa pratensis, Madia spp., Hypericum perforatum, Geranium dissectum, Sidalcaea campestris and Carex tumulicola* (Frenkel and Streatfeild 1994).

Within the lower lying intermound areas, herbs are important. Often submerged during the peak precipitation in winter and early spring months, water tolerant species dominate intermounds. Unlike the mounds, the intermounds favor perennial forbs (55.0%) and native species dominate (73.1%). Key intermound species include: *Deschampsia cespitosa, Beckmannia syzigachne, Hordeum brachyantherum, Plagiobothrys scouleri, Juncus spp. and Carex spp.* (except *C. tumulicola)* (Frenkel and Streatfeild 1994).

Differences between research units are apparent both in the field and on low altitude aerial photographs. The above mentioned differences between mound and intermound plant communities exist, to a differing degree, in each of the treatment spaces. Space 1, burned

annually, is generally more open than the other spaces. Except for *Spiraea douglasii* , bunch grasses dominate. The woody vegetation associated with the higher mound areas has a low stature and is limited mostly to rose. Single ash and small stands of hawthorn are present. Topographic pattern expressed by vegetation is most apparent in Space 1.

Space 2, the control area, again exhibits the general mound-intermound species differentiation. Due to the absence of fire, rose and spiraea have formed large, dense, often impenetrable woody thickets that obscure the underlying topographic pattern.

At the time of my research in 1993, Spaces 3 and 4, which are burned triennially, had only been burned in 1991. The intermound areas were generally open and dominated by graminoids. The mound areas were denser with more woody vegetation but not as mature or congested as in the control unit. Although less so than in Space 1, the differences of mound-intermound vegetation communities are apparent on the aerial photograph.

As suggested by prior research, fire history is an important control of vegetation composition (Johannessen, et al. 1971., Frenkel and Streatfeild, 1994., Towle, 1979.) With the advent of annual and triennial burning in the RNA, species richness increased while local structural diversity decreased (Frenkel and Streatfeild 1993, 1). Frenkel and Streatfeild (1991) found that individual species displayed poor correlation with burning history. Contrary to what was expected, Frenkel and Streatfeild's 1993 results found that annuals generally increased with burning while perennials decreased. This may be primarily a short-term result due to a large seed bank of alien annuals on site and a seasonal effect as 1992 was warm and dry, favoring annuals (Frenkel and Streatfeild, 1993, 4). *Rosa eglanteria* exhibited a decrease with burning yet *Deschampsia cespitosa* did not show a marked increase (Frenkel and Streatfeild 1994). Restoration to native prairie conditions is more easily achieved in the intermound areas (Frenkel and Streatfeild 1993).

METHODS

General Approach

This paper is primarily a methodological study of applying geographic techniques to an on-going biogeographical study. This study had three objectives: (1) defining the location and boundaries of treatment spaces and sampling plots in a standard geographic coordinate system, (2) delineation of spaces and plots onto a scanned image creating a spatial data base and (3) classification of vegetation and associated microtopography.

To achieve my final objective of mapping the vegetationally associated mound-intermound micro-topographic pattern, a central question of this research became whether or not the spectral information contained in the available monochromatic digital image was an indicator of vegetation and microtopography and would provide statistical differentiation of class signatures necessary for accurate digital image classification.

In my attempt to digitally classify the image based on signatures developed from the single band, I made the following assumption: that the principles and techniques of remote sensing and image processing traditionally used with small scale imagery could be applied to large scale imagery of a small research site.

I hypothesized that, (a) mound and intermound vegetation differences in structure, texture, and composition would be represented by spectral differences, and (b) these spectral differences of micro-topographic class association would be statistically distinct. It would then follow that digital image classification would be possible based on signature sets developed from training plots of known vegetation type.

Ground Point Location

The Oregon State University Department of Geosciences' newly acquired Trimble Navigation Global Positioning System (GPS) was used to establish the location, recorded in Universal Transverse Mercator (UTM) coordinates of the following:

(1) ground control positions for digital image rectification;
(2) control positions to aid in the digitization of the RNA boundary and treatment units; and
(3) positions of 38 vegetation plots and 6 older research plots established in 1983.

The GPS was selected based on the following attributes: (a) use by a single operator, (b) positional data is recorded in digital format using UTM coordinates, (c) ability to collect real-time positions quickly and accurately, (d) ability to record positions in the open prairie environment lacking abundant visually identifiable reference points, and (e) ability to record positions independent of each other. This last point is an advantage in the RNA where distances between positions were large.

The Global Positioning System, developed and operated by the United States Department of Defense, is a system for navigation and measuring locations upon the earth's surface. Based on traditional principles of navigation a constellation of 24 high-altitude satellites orbiting the earth broadcast signals which are picked up simultaneously by a stationary receiver, in this case, the Community Base-station located on the roof of Wilkinson Hall, Oregon State University, Corvallis and the mobile field receiver. The main functions of the GPS are data capture and navigation (Hurn 1989). For this project, ground point location data capture was used. To increase the accuracy of position data, raw points were subjected to differential correction using Trimble Navigation software allowing for accuracy in the sub-meter range.

Equipment:

- Field notebook
- 1992 black and white, low altitude aerial photograph of the RNA
- Trimble Navigation Pathfinder Basic receiver (Rover 5.29) with external antenna, tripod and battery pack
- Trimble Navigation post-processing software (PFINDER 2.2) and IBM 386 computer
- Community Base-station positional data (PFINDER 2.2)

Prior to conducting field work, rover data collection parameters were selected. Informational parameters define the manner in which data will be *displayed* and include: Dynamic Code, Altitude Reference, Datum, North Reference, Units of Measurement, Coordinate System and Time Zone. Critical parameters, defining how the data will be *collected* include: Positional Fix mode, Percent Dilution of Precision (PDOP) mask, PDOP switch, Elevation mask, Signal to Noise Ratio (SNR) mask, Filter Coefficient and Position Logging Interval. Selection of critical parameter settings was based on the advice of Trimble Services personnel, Trimble operating manuals and a bit of best guess/trial and error. GPS parameter settings used for this project are listed in Appendix 2.

Prior to beginning each GPS field day, a preliminary reading was recorded at the United States Geological Survey (USGS) Global Positioning Super-station marker E141 located along the southern boundary of the RNA, approximately three quarters of a mile west of U.S. Highway 99W. Readings at this USGS precisely located and recorded position provided a pre-field test of the equipment, daily conditions, and an accuracy check of differentially corrected data of this known location as an estimate of the accuracy of subsequent readings.

Field location readings were recorded for the northwest corner of each of the 38 vegetation plots, at least one corner of the six older research plots and 13 ground control points at strategic locations on the perimeter of the RNA. All readings were conducted with the rover mounted on a tripod, and connected to an external antenna balanced at two meters above ground level. Positional readings were taken at one second intervals for at least five minutes to include at least 180 sample point readings. During the recommended three minute warm-up period for the rover, pre-reading information was recorded which included: the file number, field location, number of satellites available, the PDOP, accuracy level and a check that the reading could be made in 3D. If the number of satellites was low (less than 5) or if the PDOP was higher than 6.0, field work was halted for the day. This same information, along with the duration of data collection and the number of data points collected, was recorded at the end of each reading. This process was repeated at each of the postional fix sites (Appendix 3).

Postional data were downloaded from the rover onto a 386 computer for differential correction using Trimble Navigation post-processing software. Accuracy was increased by normalization of positional data using statistical corrections of the constant Base-station known position and the satellite positional data which the Base-station receive and records. From this statistical data base, a mean center location was calculated for the sample points in UTM units.

Data Base Development

Creation of the digital data base was essentially a four step process which included:

1. Importation of the Tagged Interleaved File Format (*.tif) digital image file into IDRISI image (*.img) format
2. Rectification and georeferencing of the digital image
3. Creation of vector files for RNA boundary and Spaces 1-4
4. Creation of vector files for vegetation plots

These steps created the primary data base which was then used in conjunction with image classification techniques to create the final thematic map.

Equipment:

- IDRISI Image Processing/Geographic Information System software (version 4.1)
- Digital, low altitude, true color, 1993 aerial photograph of study site: scanned as a single band, 8-bit, 1724 rows x 2298 columns, 1.2 meter pixel resolution
- USGS Greenberry, Oregon 1:24,500 topographic map
- 1991 black and white, low altitude, aerial photograph of site
- Differentially corrected GPS location data for ground control points and vegetation plots

Digital color imagery, rather than low altitude black and white photography was utilized to (1) create a GIS/digital image data base and (2) test the utility of delineating mound-intermound micro-topography for the region based on digital classification of vegetation communities defined by vegetation sampling field data. The digital aerial photograph of the site was purchased from the Western Aerial Corporation (WAC) of Eugene. This image had been produced by scanning the masked study area from a larger aerial color positive print. The original color positive was taken using Kodak 2445 Aeriocolor negative film and a WILD camera with a focal length lens of 213.67 mm. Flying height of the camera was 16,500 feet above ground level. The original photograph was at a scale of 1:24,000. The final image acquired had many suitable characteristics such as no striping, minimal distortion from roll, pitch, yaw, and vignetting, and was acquired on a cloud-free day. The spatial resolution of the imagery, 1.2 meter pixels (picture element or unit of resolution), was appropriately fine for the research design.

Scanning the photograph into digital form was conducted by WAC using a single pass Agfa scanner (FotoLook V1.26). Adobe Photoshop software was used to create a single band, 8-bit per pixel color index image from the initial 3 band, 24-bit per pixel scanned image. The 8-bit image is monochromatic with pixel values ranging from 0-255.

Rectification and Georeferencing

IDRISI software has a simple conversion command allowing for importation and conversion of Tagged Image File Format (*.tif) files into IDRISI readable image (*.img) files. After reformatting, rectification and georeferencing were conducted. Rectification is the process of fitting the data to a map projection or grid system. Resampling is the means by which data values are extrapolated from the original source grid to the new grid/projection. The process of assigning map coordinates to the image is referred to as georeferencing.

Initially 13 ground control points were selected from the 1991 black and white aerial photograph, distributed along the perimeter of the RNA, and distinguishable on both the photograph and in the field. Difficulty in selecting ground control points due to: (1) the scale difference between the photograph and the pixel resolution of the digital image and (2) the one year difference between the photograph and the digital image, led to the dismissal of four of the original 13 points. A first order (linear) polynomial fit using a nearest neighbor resampling technique for a RMS error of 2.72 pixels (+/- 3.26 meters) was selected as it requires the least number of control points (three required) and retains much of the original data integrity. Six control points remained after three points with high RMS error were removed during the rectification process.

The final ground control points were not evenly distributed along the perimeter and tended to be located in the northern and eastern regions of the RNA boundary due to the lack

of distinguishable features in other areas of the digital photo. As a result, potential distortion is both increased and concentrated outside of these areas of the image. Nonetheless, the distortion effects seemed to be minimal as the overlay of GPS positions on the georeferenced image show little displacement from their original positions.

Creation of Vector Files

Following georeferencing, vector files defining the RNA boundary, burn units (Spaces 1-4) and vegetation plots (1-36, 5a and 18a) and six past research plots were created. Boundary and research space vector files were built using a combination of differentially corrected GPS perimeter points and on-screen digitization with the aid of the 1991 hard copy black and white photograph for boundary attribute recognition. Vegetation plot vector files were created using the differentially corrected GPS position acquired for the northwest corner marker of each of the 38 vegetation plots. From this corner point position the three remaining corner point positions for each plot were calculated by adding 25 meters at 90 degree angles, yielding a 25 meter square area for each plot. This same procedure was followed for the six older 450 foot square research plots.

Digital Image Classification

Three stages are involved in the supervised classification process: training, classification and output (Lillesand and Kiefer 1979, 669). Training involves defining regions of the image that represent the output classification categories. Training areas should be as homogeneous as possible and exhibit unimodal frequency distributions in each of the bands used (Campbell 1987,314).

A signature is a statistical description of a class from these training areas combined over all input bands. During classification each pixel (picture element or cell of resolution) in the image is statistically compared to the signatures and then assigned to a class.

Procedure:

- Creation of Relative Richness image
- Division of image into research sub-spaces
- Digitization of training sites
- Development of training signatures
- Examination of pre-classification training statistics
- Application of classification routine using (a) Maximum Likelihood Classifier and (b) Minimum Distance to Mean Classifier upon selected bands
- Recombining of classified research sub-spaces into single thematic maps
- Extraction of classification results
- Final cartographic output

Creation of Relative Richness Band

Traditional image classification relies on the use of either a single band or a set of bands of reflectance data, each limited to a narrowly defined region of the electromagnetic spectrum. Signature differentiation can often be effectively increased through the use of multiple data sources provided by additional bands of data. Therefore, a second image was created in order to test the effectiveness of signature differentiation with additional information provided by a second band of data.

The visual distinction between mound and intermound topographic patterns on the digital image is a result of reflectance differences in the visible bands due to the color, physiology, phenology and density of the associated vegetation. Distinction in mound/intermound community structure and composition is revealed by both vegetation analysis and digital analysis of the vegetation polygons extracted from the original image.

The PATTERN module within IDRISI uses variability within a 3x3 pixel moving window to assess a variety of pattern measures commonly used in landscape ecology. To investigate signature distinction based upon patterns within the micro-topographic communities the Relative Richness index was selected to create a pseudo-band. Relative Richness is the variability of pixels within the 3 x 3 window as a percentage of maximum variability possible (R=n/nmax*100, where n= number of different classes present). Output from the module is a new image where the new pixel value is resultant of the pattern index selected upon the original value.

Because the numeric results of the index were narrow, a multiplier of 63 was applied to the resulting image extending the digital range as close as possible to the 0-255 range achievable with 8-bit data. Classification routines later applied to the data require the input of byte binary data. Therefore, data resultant from the Relative Richness index was truncated to whole numbers.

Treatment Space Division

Prior to each classification, four separate images, each consisting of one of the four research spaces, were masked from the original and Relative Richness images. Because of its similar burn history the undesignated area to the west of and contiguous to Space 2 was included as part of Space 2 for classification purposes. Digital numbers outside the research areas were reset to zero. This allowed for each of the treatment areas to be classified separately. Once classified, the separate images of the treatment areas were merged to form a single image consisting only of areas within the RNA study site.

Pre-classification separation of research areas was conducted for two reasons. First, it eliminated classification of areas within the image yet outside of the study area. Second, as

was discovered during a pre-test using the maximum likelihood classification routine on the full-scene original single band image, failure to do so resulted in classification error. The eight signatures, based on all burn history and topographic combinations, were inseparable. This was due to the limited information contained in the single band. For this reason, *a priori* knowledge of burn history was used to eliminate the need for between space signature development and classification distinction.

Development of Training Site Vector Files

Supervised classification relies on the availability of *a priori* knowledge of the study site so that training sites can be established from ground locations of known characteristics. Therefore, 36 of the 38 vegetation sampling plots were used as training sites for the mound-intermound classification of the RNA. Plots 2 and 5A in Space 1 were not used because of their location on a mound-intermound fringe. This made them difficult to classify into either topographic type based on statistical analysis of vegetation association or wetland species association index (Frenkel and Streatfeild 1994).

Signature training sites for supervised classification were created within the boundaries of the 36 research vegetation plots. Signature training sites are samples of the desired classification categories. Digital numbers in each site are used to develop signature statistics. These signatures are then analyzed, edited if need be, and used to classify the remaining area of the image into one of the signature classes.

Training sites were created within the vegetation plots for two reasons. First, Frenkel and Streatfeild (1994) had previously classified these sites as being of either mound or intermound topography based on field observations of the plots, vegetation associations and original aerial photographic selection of plot location by strata association. Second, the

extraction of statistics from a sub-space within each of the research plots allowed classification accuracy to be established by examining classification results from the area within the plots but not included in the development of training signatures.

Polygon files for training statistic development were created by on-screen digitization. Using guidelines digitized from the upper left to lower right and the upper right to lower left corners of the plot, an **X** shape polygon of approximately four pixels width was digitized for each vegetation plot (Figure 4). Final training sites encompassed approximately 27% of the area within vegetation plots for each topographic class per space.

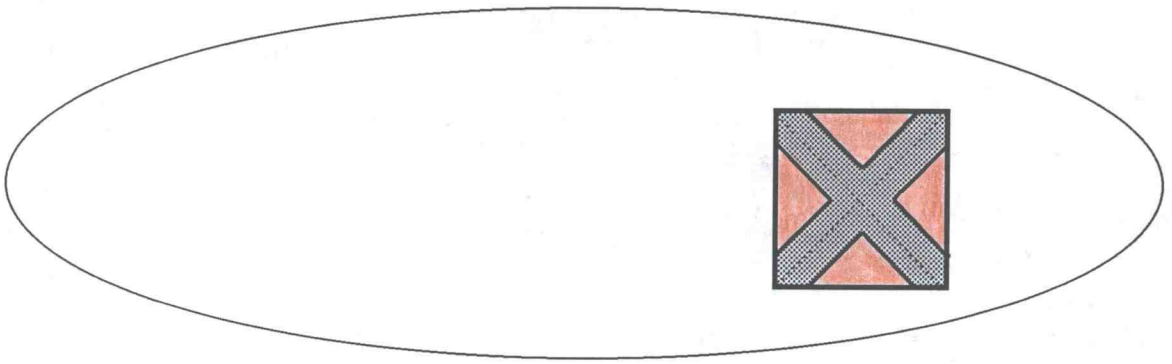

Figure 4. Schematic of a mound associated vegetation plot (bold line), guidelines (dotted line) and digitized training areas (grey area) used for signature development. Classification accuracy assessment was based on the area lying within the vegetation plot polygon yet not included within the signature training area (red area).

Mound-Intermound training sites and plot assignments were:

Space 1	Mounds: 3, 4, 5, 8 Intermound: 1, 6, 7, 9, 10
Space 2	Mounds: 14, 15, 16, 17, 18, 18a Intermounds: 11, 12, 13, 19, 20
Space 3	Mounds: 21, 22, 24, 29, 30 Intermounds: 23, 25, 26, 27, 28
Space 4	Mounds: 32, 33, 34 Intermounds: 31, 35, 36

Development of Training Signatures

Signature training polygons were classed according to micro-topographic association (mound or intermound) within a separate polygon file for each of the burn treatment and control spaces (Spaces 1-4). Signatures were created for micro-topographic association based on the original and Relative Richness pseudo band. This yielded four signatures per treatment space.

Application of Classification Routine

Three classification strategies were applied: (1) signatures developed from training sites taken from the original image were used to classify the image using IDRISI's maximum likelihood routine and (2) minimum distance supervised classification routine, (3) signature sets from the original and Relative Richness images were used in combination with the maximum likelihood routine.

The use of the minimum distance and maximum likelihood classifications with training statistics from the original single band data allowed for comparison between classification routines. The maximum likelihood routine using the combined training statistics of the original and Relative Richness images allowed for the assessment of additional bands of data created from a single data source as a means of increasing signature differentiation.

Maximum Likelihood Classifier. This classification routine was performed using signatures based on the original single band, 8-bit image, and with the combined original and Relative Richness signature sets. While computationally demanding, an appealing attribute of the maximum likelihood classifier is its ability to take into consideration both statistical variation within a class and overlap of the digital number frequency distributions of classification categories. By taking into account the mean and the variance or variability of values within

each class, this classifier is better able to discern the membership and class association of "maximum likelihood". Because of this ability it is also very sensitive to the quality of the training data and is based on the assumption of normality of the frequency distribution of pixel values within each training class (Campbell 1987, 320).

The maximum likelihood routine in IDRISI allows the user to employ *a priori* knowledge about the site in question by permitting the user to either specify the probability of pixel inclusion in a class based on the expected class coverage or to assume equal class probability. For this application equal probability of mound versus intermound association was chosen. Additionally, the routine allows the user to specify what percent of the pixels least likely to belong to the categories in question are to be left unclassified (either 0%, 1%, 5% or as a chi-square statistic). In order that only the most probable pixels be classified and therefore reduce misclassification, the least likely 5% were selected to be unclassified.

Minimum Distance (to mean) Classifier. The minimum distance classification routine was performed on the original single band image. This type of classification is one of the more mathematically simple and computationally efficient routines but has limitations. Pixel classification is based on the distance between the mean of the training plot digital numbers and the digital number of the pixel to be classed. Unlike the maximum likelihood classifier, this routine does not consider statistical variance within classes. Thus, reliability is lacking in cases where spectral classes are close or overlapping and have a high level of variance (Lillesand and Kiefer 1979, 673).

Within this classification module IDRISI has two methods for calculating distance to the mean: raw distances or distances normalized by the standard deviation in each band under consideration. In either case the user must specify the maximum distance beyond which a pixel will be left as unclassed (zero). The IDRISI manual suggests that distances in standard

deviations should have superior performance when a large number of training pixels are used. It was assumed that training areas for this project had a sufficient number of pixels (428-1033 per signature); therefore, 1.96 standard deviations, or 95% of those pixel values closest to the mean, were selected to be classified.

Cartographic Output

Based on accuracy assessment comparisons, the single band maximum likelihood classification was selected for final cartographic output. To reduce noise and smooth fragmentation, a moving 3x3 pixel mode filter was passed over the maximum likelihood output image using IDRISI's FILTER module. To add text and color print maps, IDRISI image files (*.img) were reformatted (*.tif) and imported into ARCINFO's GRID module. Once transformed into a grid format the images were displayed in ARCPLOT and titles, neat lines and legends were added to prepare the maps for printing. ARCPLOT compositions were then converted to Postscript format and printed on a Colorcal Postscript printer.

RESULTS

Global Positioning System

Average differences between the pre-field collection GPS tests and the USGS defined position of the Super-station were sub-meter in the easting reading at 0.93 meters and 1.47 meters in the northing measurement. The minimum difference was 0.29 meters in the northing and 0.01 meters in the easting. Maximum difference in the northing was 2.54 meters and 1.97 meters in the easting. From these test readings taken prior to each GPS field period, it can be assumed that subsequent field positions were at this level of accuracy.

Use of differentially corrected GPS positions as ground control points yielded a georectified image with an postional error of 3.26 meters (RMS 2.74). Accuracies of the differentially corrected GPS positions (+/- 2.54 meters) and georeferencing process (+/- 3.26 meters) were also evident when the differentially corrected field positions were placed upon the georeferenced image. Corrected GPS positions were within 1-3 pixels (+/- 1-4 meters) of the feature locations observable upon the image.

Appendices 4 and 5, respectively, record the differentially corrected GPS locations in UTM units of the 38 permanent vegetation plots and six 1983 research plots with a locational accuracy of +/- 2.54 meters. This accuracy estimate is based on differentially corrected GPS readings of the USGS Super-station. Also shown are the number of samples recorded and the standard deviation of the samples. Appendix 6 records the differentially corrected GPS positional reading in UTM units taken prior to each GPS field day at the USGS Super-station marker.

Pre-Classification Vegetation Sampling Plot Characteristics

Table 1 provides micro-topographic class spectral reflectance statistics for the original single band, 8-bit image as derived from the 36, 25 meter square, vegetation sampling plots distributed in each of the four research spaces. Extracted plot data were combined according to micro-topographic class and research space association. Statistics include the spectral reflectance mean and standard deviation for each micro-topographic class per research space. Also included are the range of values (highest digital number minus lowest digital number), the number of different digital numbers present (digital diversity), and the number of pixels representing each micro-topographic/treatment space category. Difference values between the mound and intermound statistical characteristics are also shown for each of the research spaces.

Within-space mean reflectance value differences between micro-topographic classes are moderate, and especially low within Space 3. Standard deviations for micro-topographic classes within all spaces are relatively high but tend to be higher for intermounds than for mounds.

The digital diversity (number of different digital numbers present) of the mound and intermound vegetation sampling plots may be an indicator of textural heterogeneity reflecting structural and species diversity. Spaces 1 and 3 exhibit large differences in digital diversity between micro-topographic classes (24 and 29 respectively) while Spaces 2 and 4 show rather low differences (3 and 5 respectively).

Table 1. Research space statistics derived from vegetation sampling plots for original single band, 8-bit image.

	Mean	Standard Deviation	Range	Digital Diversity	Sample Size (pixels)
Space 1 Mound	149.47	17.95	168	62	2206
Space 1 Intermound	126.59	32.62	235	86	2904
Difference	22.88		67	24	693
Space 2 Mound	153.92	14.53	120	53	3552
Space 2 Intermound	117.02	26.87	192	50	2904
Difference	36.90		72	3	648
Space 3 Mound	162.43	9.47	74	27	2904
Space 3 Intermound	162.30	21.23	182	56	2880
Difference	0.13		108	29	24
Space 4 Mound	160.15	9.97	67	24	1727
Space 4 Intermound	142.83	14.86	93	29	1728
Difference	17.32		26	5	1

Table 2. Training site statistics for original single band, 8-bit image.

	Mean	Standard Deviation	Range	Digital Diversity	Sample Size (pixels)
Space 1 Mound	147.32	19.32	135	40	645
Space 1 Intermound	126.62	32.38	189	63	834
Difference	20.70		54	23	189
Space 2 Mound	153.36	14.73	109	42	1033
Space 2 Intermound	117.05	27.30	192	40	757
Difference	36.31		83	2	276
Space 3 Mound	162.18	9.26	73	22	827
Space 3 Intermound	161.77	21.68	182	44	803
Difference	0.41		109	22	24
Space 4 Mound	160.40	10.02	67	25	454
Space 4 Intermound	142.51	15.10	81	24	428
Difference	17.89		14	1	26

Table 3. Training site statistics for Relative Richness pseudo-band.

	Mean	Standard Deviation	Range	Digital Diversity	Sample Size (pixels)
Space 1 Mound	116.65	34.16	177	8	645
Space 1 Intermound	133.95	34.64	177	8	834
Difference	17.30		0	0	189
Space 2 Mound	112.46	34.98	202	9	1033
Space 2 Intermound	111.69	30.45	177	8	757
Difference	0.77		25	1	276
Space 3 Mound	86.55	24.54	151	7	827
Space 3 Intermound	110.27	32.34	202	9	803
Difference	23.72		51	2	24
Space 4 Mound	91.80	25.89	151	7	454
Space 4 Intermound	110.72	30.76	152	7	428
Difference	18.92		1	0	26

Training Site Statistics (signatures)

Tables 2 and 3 record the mean, standard deviation and number of pixels included within each of the micro-topographic signature training sets per research space for both the original image (Table 2) and the Relative Richness image (Table 3). Additionally, digital range and diversity are recorded. Difference values between class signatures for each of the above statistics are shown for each research space as in Table 1 for the original image.

While smaller than the vegetation plots from which they were extracted, the signature training sets maintain similar spectral reflectance characteristics. Again, within-space micro-topographic class reflectance differences are moderate and especially low within Space 3 (0.41). Standard deviations within all spaces are relatively high. Signature class differences in digital diversity are large in Spaces 1 and 3. Low differences in digital diversity are found in Spaces 2 and 4 (Table 2).

Signature training sets derived from the Relative Richness image also exhibit moderate mean reflectance value differences and high standard deviations for the micro-topographic classes (Table 4). Unlike the original data set, it is in Space 2 that the mean reflectance value difference is extremely low (0.77) while Space 3 signatures display the greatest difference in class means (23.72). Because of the generalizing effect of the Relative Richness filter, the difference in the number of digital numbers present in each class is rather low (Table 3).

Vegetation Plot and Training Site Histograms

Figures 5 through 7 display spectral reflectance value histograms for mound and intermound micro-topographic type as expressed by vegetation plots and the sub-plot training sites for each of the research spaces from the original and Relative Richness images.

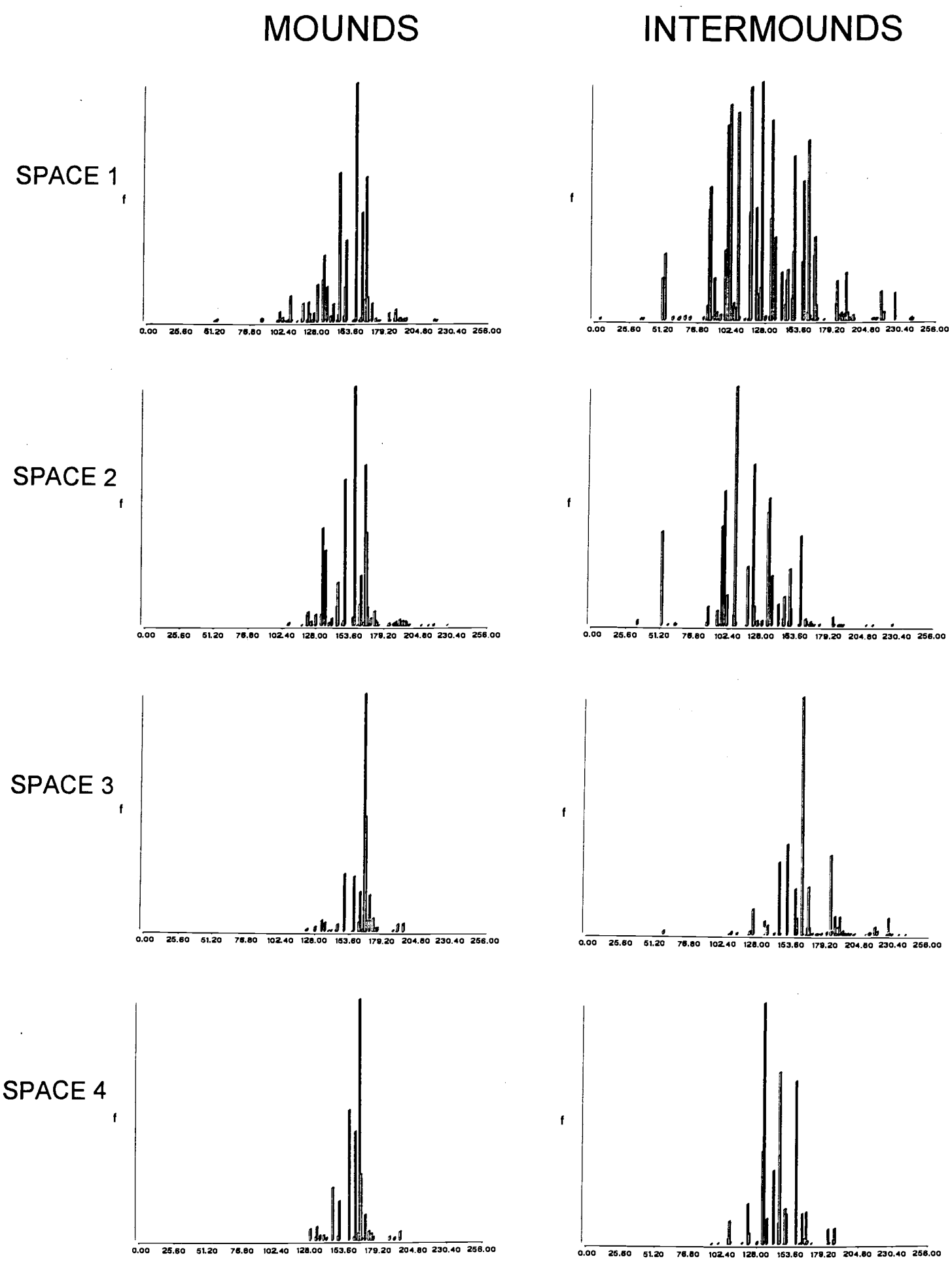

Figure 5. Histograms of digital numbers representing vegetation plots masked from the original single band image.

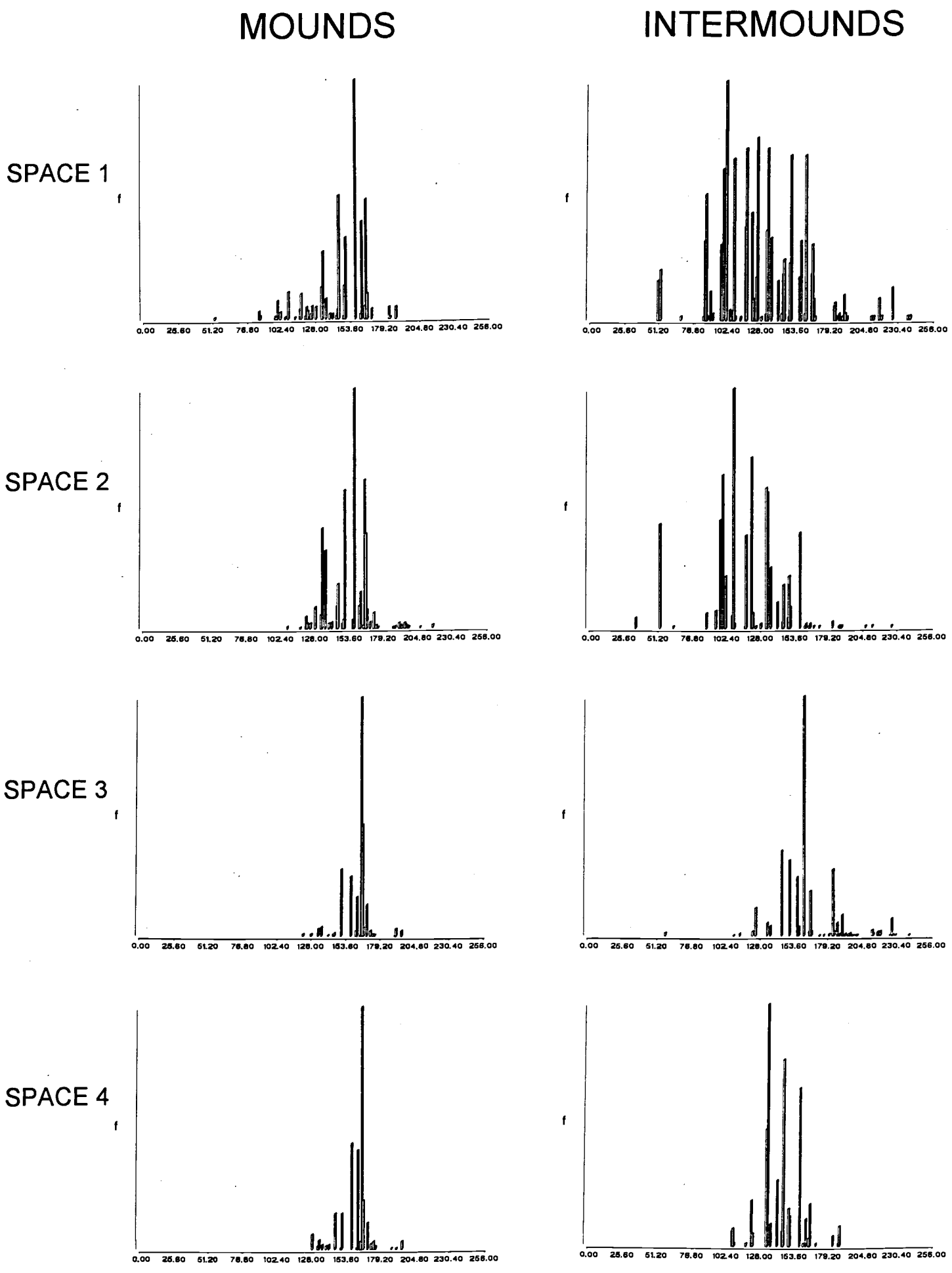

Figure 6 Histograms of digital numbers representing class signatures from training plots masked from the original single band image.

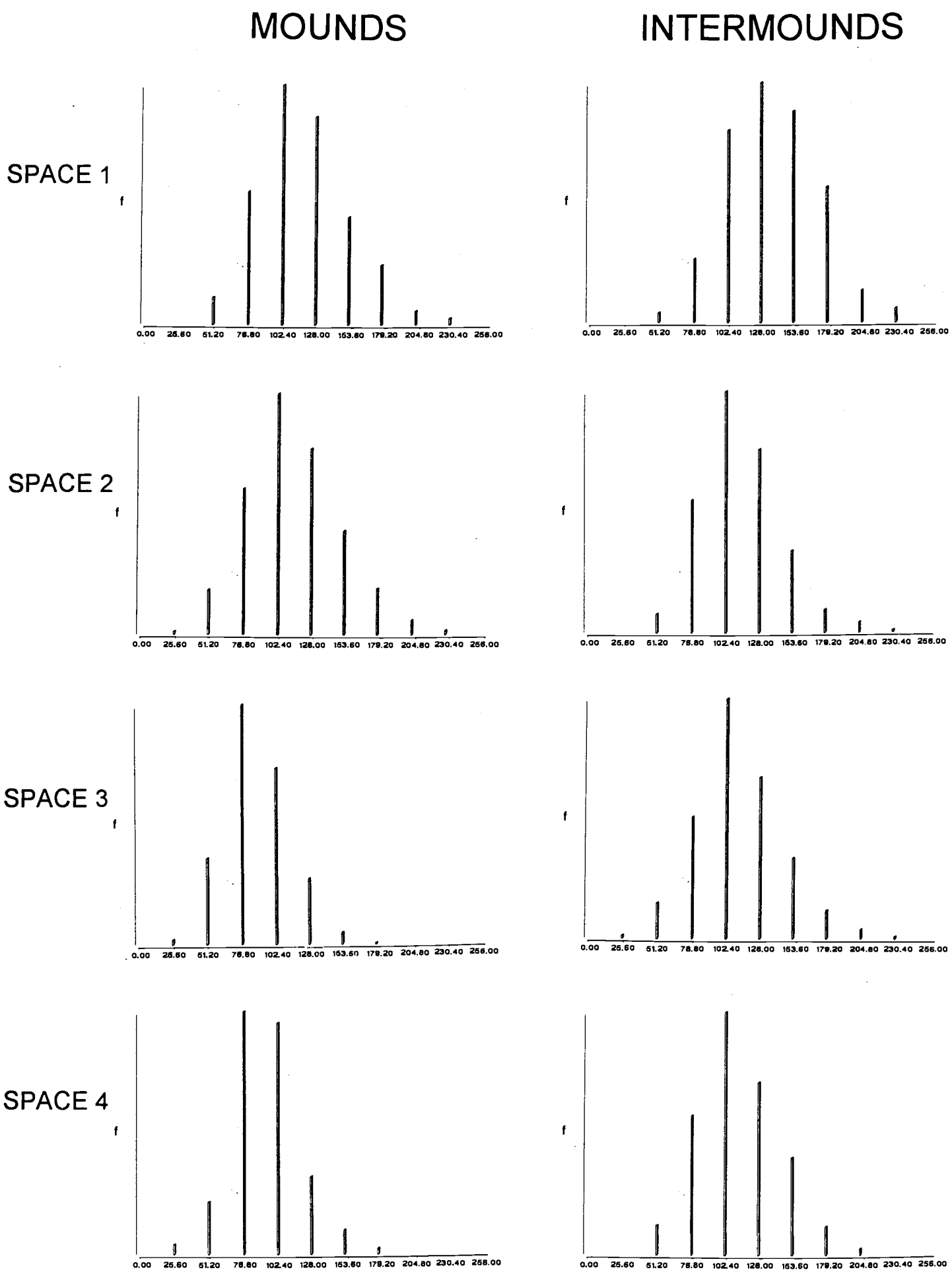

Figure 7 Histograms of digital numbers representing class signatures from training plots masked from the Relative Richness pseudo image.

In comparing spectral reflectance histograms based on the original digital image it is evident that the training sites (Figure 6) closely approximate the mean, range, and general distributional shape of the vegetation plots (Figure 5) from which they were sub-set. Important differences between micro-topographic class spectral data include the range and normality of distribution. Frequency distributions of digital numbers extracted from mound regions are narrower, representing less deviation from the mean and a smaller value range than those of intermounds. The range of the mound data often intersect the range of the intermound data. It is evident that there is slight bimodality to the distribution of the intermound data. This is especially true for Spaces 1 and 2. The greater range, deviation and diversity of digital numbers of Space 1 intermounds probably reflects the controlled burn 9 months prior to the image date. The uneven spread and intensity of the burn created a diversity of surfaces and textures with exposed soil, charred vegetation, re-growth, and unaffected older growth all present in the area. These differences in signature characteristics are important in assessing both the classification technique used and the results achieved.

Figure 7 displays training site histograms from the Relative Richness pseudo-band. Because of the generalizing effect of the Relative Richness algorithm, these histograms are smoother in appearance, display a more normal distribution, and are comprised of fewer digital numbers.

Image Classification Accuracy Assessment

Classification accuracy assessment results are presented in Table 4. Results are separated by classification routine and bands used in the classification process. Results are based on the total number of pixels within the accuracy assessment area (within vegetation

Table 4. Classification assessment of vegetation plots based upon the size of the training sample by space and by topographic class.

MAXIMUM LIKELIHOOD CLASSIFICATIONS:

Training Signatures and Classification based upon Original 8-bit Band Values:

	MOUND			INTERMOUND			AVERAGE PER SPACE		
	CORRECT	ERROR	UNCLASS	CORRECT	ERROR	UNCLASS	CORRECT	ERROR	UNCLASS
SPACE 1	89.74%	7.62%	2.65%	53.72%	39.86%	6.43%	68.91%	26.26%	4.83%
SPACE 2	83.72%	13.10%	3.18%	71.97%	20.63%	7.41%	78.31%	16.57%	5.12%
SPACE 3	92.20%	7.80%	0.00%	34.81%	59.94%	5.25%	63.51%	33.87%	2.62%
SPACE 4	85.13%	13.06%	1.81%	68.46%	25.31%	6.23%	76.70%	19.25%	4.05%
AVE. PER CLASS	87.58%	10.48%	1.94%	56.23%	37.42%	6.35%	**71.68%**	**24.15%**	**4.17%**

Training Signatures and Classification based upon Original and Relative Richness Band Values:

	MOUND			INTERMOUND			AVERAGE PER SPACE		
	CORRECT	ERROR	UNCLASS	CORRECT	ERROR	UNCLASS	CORRECT	ERROR	UNCLASS
SPACE 1	80.93%	14.64%	4.44%	52.75%	33.43%	13.96%	64.64%	25.50%	9.86%
SPACE 2	76.06%	19.33%	4.61%	74.71%	16.35%	8.94%	75.44%	17.96%	6.60%
SPACE 3	87.53%	12.37%	0.10%	45.84%	46.51%	7.66%	66.68%	29.44%	3.88&
SPACE 4	81.90%	15.42%	2.68%	68.54%	24.46%	7.00%	75.15%	19.99%	4.86%
AVE. PER CLASS	81.29%	15.74%	2.97%	59.77%	30.64%	9.59%	**70.38%**	**23.30%**	**6.33%**

MINIMUM DISTANCE CLASSIFICATION:

Training Signatures and Classification based upon Original 8-bit Band Values:

	MOUND			INTERMOUND			AVERAGE PER SPACE		
	CORRECT	ERROR	UNCLASS	CORRECT	ERROR	UNCLASS	CORRECT	ERROR	UNCLASS
SPACE 1	73.11%	25.63%	1.25%	67.10%	27.10%	5.80%	70.64%	26.48%	3.88%
SPACE 2	76.26%	20.56%	3.18%	76.62%	15.98%	7.41%	76.43%	18.45%	5.12%
SPACE 3	0.00%	100.0%	0.00%	94.75%	0.00%	5.25%	47.38%	50.00%	2.62%
SPACE 4	79.86%	18.33%	1.81%	71.31%	22.46%	6.23%	75.54%	20.42%	4.05%
AVE. PER CLASS	55.25%	43.58%	1.65%	78.08%	15.75%	6.18%	**66.83%**	**29.46%**	**3.95%**

sampling plot yet not included within the training site for signature development) per topographic class for each research space.

"Correct" values are the percentage of pixels within the accuracy assessment area per topographic class and classified as such by the classification routine per space. "Error" values are the percentage of pixels within the accuracy assessment area per topographic class per research space that were misclassified as a result of the classification routine. It is important to note that misclassification of one class results in over representation of the other. This type of error is not accounted for in the accuracy assessment of the over represented class. "Unclass" is the percentage of pixels that remained unclassified after the classification was performed.

Research space averages (right hand column) are based on the total number of pixels within the accuracy assessment area of both the mound and intermound topographic class per space. Mound and intermound topographic class averages (bottom row) are based on the total number of pixels within the accuracy assessment area for all spaces per topographic class combined. Final averages (bottom row, right, bold) are based on the number of pixels within all assessment areas classified as correct, error or unclassified for the total number of assessment pixels.

Table 4 shows that when using the maximum likelihood classifier, mounds tended to have higher correct averages than the intermounds. Using signatures based on the original image, mounds classified correctly at an average of 87.58% while intermounds correctly averaged at 56.23%. Error in intermound classification is especially apparent in Space 3 where correct classification was only 34.81%. Using signatures based on both the original and Relative Richness band also produced better results for the mounds at 81.29% as compared to the intermounds at 59.77%. Thus, while the addition of the secondary data band increased the accuracy of intermound classification, primarily due to the increased accuracy of

intermound classification within Space 3, it was at the expense of the accuracy of the mound classification.

The minimum distance routine had the highest percent correct average (78.08%) for intermounds. Yet, it can be seen that this was at the expense of the accuracy of the mound classification, which achieved an overall accuracy of only 55.25%, due to the extreme classification error associated with Space 3.

The overall highest percentage of correctly classified pixels for both topographic classes within all spaces resulted from signatures based on the original image using the maximum likelihood routine (71.68%). The greatest overall error occurred using the minimum distance algorithm (29.46%). The largest percentage of pixels left unclassified were a result of the combined original and Relative Richness signature sets using the maximum likelihood classifier (6.33).

Table 5 lists plot level accuracies achieved when using the maximum likelihood classifier and training plots from the original image, which had resulted in the highest overall accuracy as outlined in Table 4. Mound plots had generally high accuracies with 15 of the 18 mound designated plots achieving classification accuracies of +80%. Plots 17 and 18a in Space 2 and plot 21 in Space 3 classified less than 80% correctly. Intermounds plots are more variable and less successful in their classification success rate. Five of the 18 intermound plots achieved +80% correct classification. Of the 13 plots classifying less than 80% correctly, eight classified below 50% correctly and include all intermound plots located in Space 3, plots 7 and 9 in Space 1, and plot 20 in Space 2.

Table 6 lists the post classification percentages of total area classed by topographic type or left unclassified for each space according to classification routine and bands used in the classification process. Results show that regardless of the classification algorithm used, a higher percentage of all spaces is classified as mound. The minimum distance routine tended

to assign more area to intermounds while the maximum likelihood classifier assigned a higher percentage of area to mounds. Maximum likelihood classification based on the two-band signature set resulted in the highest percentages of unclassed pixels.

Figure 8 is the final classification output for this study . This map was created using the maximum likelihood classification routine and signature sets developed from the original single band image. In order to achieve a smoother image and reduce noise, a 3 pixel X 3 pixel "mode" filter was passed over the maximum likelihood output image.

Table 5: Plot assessment of classification accuracy of the maximum likelihood routine based training sites form the original image. Percentages based on total pixels within the accuracy assessment area of individual plots.

Maximum Likelihood Classification: Original Image

MOUND				INTERMOUND			
PLOT	CORRECT	ERROR	UNCLASS	PLOT	CORRECT	ERROR	UNCLASS
SPACE 1							
3	95.28%	1.89%	2.83%	1	68.47%	26.82%	4.71%
4	81.63%	15.22%	3.15%	6	81.75%	15.17%	3.08%
5	94.56%	0.52%	4.92%	7	25.06%	73.29%	1.65%
8	88.12%	11.16%	0.71%	9	10.75%	77.50%	11.75%
				10	81.75%	6.75%	11.50%
SPACE 2							
14	97.40%	1.18%	1.42%	11	86.08%	9.43%	4.48%
15	91.71%	1.22%	7.07%	12	71.59%	0.00%	28.40%
16	90.25%	2.00%	7.75%	13	72.58%	25.58%	1.84%
17	67.06%	32.24%	0.70%	19	94.88%	4.65%	0.47%
18	93.72%	5.58%	0.70%	20	33.89%	64.92%	1.19%
18A	63.08%	35.05%	1.87%				
SPACE 3							
21	79.00%	21.00%	0.00%	23	34.04%	59.15%	6.81%
22	96.52%	3.48%	0.00%	25	48.18%	51.30%	0.52%
24	94.66%	5.34%	0.00%	26	17.75%	71.75%	11.0%
29	94.84%	5.16%	0.00%	27	37.70%	57.61%	4.68%
30	94.88%	5.12%	0.00%	28	37.05%	59.77%	3.18%
SPACE 4							
32	80.32%	18.29%	1.39%	31	81.34%	7.14%	11.52%
33	91.81%	5.71%	2.48%	35	74.24%	21.31%	4.45%
34	83.72%	14.68%	1.61%	36	50.11%	47.15%	2.73%

Table 6: Percent area classed as mound, intermound or unclassed per space by classification routine.

		MOUND	INTERMOUND	UNCLASSED
SPACE 1	MINDIST ORIGINAL	56.16%	40.19%	3.65%
	MAXLIKE ORIGINAL	72.90%	21.95%	5.15%
	MAXLIKE ORIG. AND RICHNESS	64.27%	26.06%	9.67%
SPACE 2	MINDIST ORIGINAL	52.58%	42.40%	5.01%
	MAXLIKE ORIGINAL	61.36%	33.62%	5.01%
	MAXLIKE ORIG. AND RICHNESS	52.69%	39.31%	8.00%
SPACE 3	MINDIST ORIGINAL	0.00%	91.36%	8.64%
	MAXLIKE ORIGINAL	58.14%	33.21%	8.64%
	MAXLIKE ORIG. AND RICHNESS	47.98%	40.53%	11.49%
SPACE 4	MINDIST ORIGINAL	46.87%	45.04%	8.09%
	MAXLIKE ORIGINAL	52.28%	39.63%	8.09%
	MAXLIKE ORIG. AND RICHNESS	49.22%	41.63%	9.15%

Note: Percent area calculations for Space 2 include the undesignated area on the western edge and contiguous to Space 2.

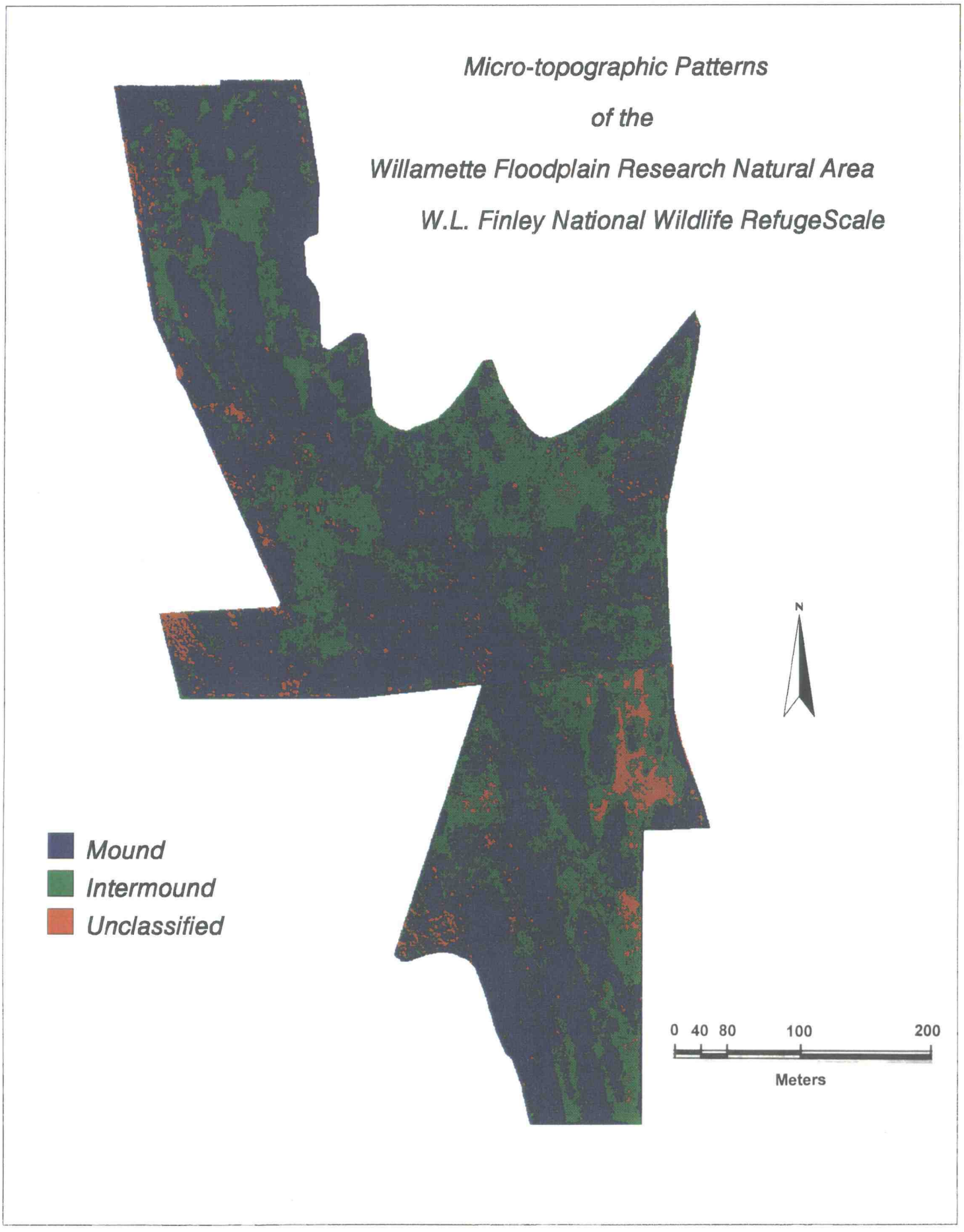

Figure 8. Maximum likelihood classification routine applied to the original single band image using training site sets extracted from within the permanent vegetation sampling plots.

DISCUSSION

Global Positioning System

The use of the Global Positioning System (GPS) in this research project proved invaluable for accurate location of ground control points used in image rectification and plots for subsequent image classification. Traditional means of geographic field mapping are often difficult, labor-and time-intensive, and require the positional reading of numerous features, some of which must also be identifiable on a second information source containing geographic coordinates. Transfer of field information onto a secondary source can also be time and labor intensive, requiring that the researcher be trained in geographic field techniques, map, aerial photograph and satellite interpretation and have cartographic skills. On the other hand, the GPS field unit is small, light weight and requires only one person to operate. In sites lacking numerous distinctive features, as was the case in this study in the open prairie of the Finley Research Natural Area, the ability of the GPS to take positional readings from any point in the field was advantageous and very time efficient. Finally, because the results of the GPS are digital and in standard geographical units (i.e., UTM coordinates), the data can be transferred directly to the digital image or to topographic maps.

Classification

The results of this classification depended on several factors: quality of the original data, accuracy in transforming the original data to a format suitable for processing, training site quality, suitability of identification classes, processing capabilities and algorithms of the image processing software, the addition of a pseudo-band as an additional source of data and finally, the interpretive skill of the analyst.

Information provided by the image, as related to the growth stage of the vegetation, is greatly dependent on image date. The May 22 date of the image used in analysis was well within the time frame of early May to late June in which plant development and photosynthesis would be at a maximum. Yet, an earlier date may have provided better distinction between topographic classes within the wetland prairie. At an earlier date, the intermounds, being at times submerged and saturated and predominately made up of annual herbs may have been more distinguishable from the perennial shrub-dominated mounds.

Limited information contained in the single band image is undoubtedly the most important factor affecting classification results. The process of aggregating three fine resolution visible reflectance channels into one wide monochromatic channel results in a loss of spectral information which would otherwise facilitate differentiation of vegetation characteristics. Because both the maximum likelihood and minimum distance algorithms classify pixels based on the mean value of the training sets, signature distinction within a single dimension becomes difficult. Maximum likelihood offers the advantage of considering both the variance and covariance of the class response patterns but assumes normality of the distributions. When applied together, the eight micro-topographic / fire regime signatures derived from the original image were indistinguishable due to the combination of similar means and large standard deviations of the signatures. Pre-classification spatial segmentation of the image into research spaces eliminated the need for signature distinction based on fire history.

Regardless of treatment space, signature differentiation between mound and intermound communities was difficult due to similarity in means and large spectral variation of intermound signatures. This resulted in moderate to complete overlap of signature classes as displayed in the digital number frequency histograms of signature training sets. Additionally, intermound signatures of Spaces 1 and 2 from the original image tend to display a histogram

that is slightly bimodal (Figures 5 and 6). Overlapping signature set distributions and similarity of class means within the single wide spectral band used in this project resulted in the misclassification of intermound areas as mounds. It is likely that those pixels spatially within intermound plots, yet having digital values both close in spectral space to the similar class means and represented within the narrow range of mound signatures, were misclassified as mound. Signature distinction within Space 3 was extremely difficult as the intermound signature completely encompasses that of the mound. The problems with signature distinction mentioned above are significantly related to the use of a single, wide, monochromatic spectral band for classification but are also related to the spectral characteristics of the micro-topographic classes and must therefore be considered in the context of the training methodology used in this research project.

Overall accuracy using the maximum likelihood routine and signatures from the original image was 71.68%, with mounds averaging 87.58% and intermound only 56.23% (Table 4). Yet, the break down of accuracies to plot level reveal that accuracies for a given region are highly variable and strongly influenced by specific plots (Table 5). Many of these low accuracies can be explained at the plot level and attributed to such factors as intra-plot heterogeneity where plots straddle the mound-intermound transition (plot 7), intra-plot heterogeneity associated with homogenous patchiness of certain species which may be uncommon to the associated class (plots 17, 20), intra-plot floristic homogeneity yet dissimilarity within a general micro-topographic class (plots 1 and 9), and intra-space class similarity probably as a function of successional stage (Space 3). Individual plot characteristics affected classification accuracies. Therefore, the issues of (1) training site quality and (2) treatment of training sites for signature development, both related to the use of pre-defined identification classes based on detailed vegetation analysis, need to be examined.

Vegetation analysis using field plots is commonly conducted in a subjective manner, or objectively using multivariate techniques. While both phytosociologists and remote sensing practitioners are interested in analyzing and ultimately documenting the vegetative landscape they differ in their approach. As noted by Treitz *et al.* (1992), phytosociologists have tended to employ objective analysis for plot classification, expounding on the repeatability and less operator bias qualities of the multivariate techniques. From the phytosociologist's perspective ground data should provide sufficient information for remote sensing vegetation mapping. Remote sensing analysts, on the other hand, have tended to favor subjective techniques, employing the use of field notes, low altitude aerial photography and ground photography to collect field data closely correlated with the spectral data (Treitz *et al.* 1992).

A comparison study conducted by Treitz *et al.* (1992) analyzed accuracies achieved using MEIS II high resolution digital imagery and supervised classification techniques with both TWINSPAN generated and subjectively defined training class sets. The researchers note that in addition to the objective, quantitative and repeatable nature of TWINSPAN, the multivariate clustering algorithm used to classify plots is similar to those used to cluster remotely sensed data. They hypothesized that supervised classification best revels ecologically important characteristics of the vegetation. Thus, objectively and quantitatively defined training classes would provide results superior to those obtained using the subjective approach traditionally employed in remote sensing vegetation mapping. Yet, their analysis found that qualitatively generated field-plot descriptions produced a more statistically accurate digital classification of MEIS II data than did detailed quantitative ground information (Treitz *et al.* 1992, 65).

Their conclusion was based, in part, on the problems associated with distinguishing classes consisting of multiple dominant species. In these cases subjective methods tend to be more monothetic and base class division on dominant species. Because the detecting

capabilities of the MEIS II sensor which, with the exception of the near-infrared band, primarily measures the top layer of vegetation, the subjective methods produced a classification scheme better suited to the spectral qualities of the image (Treitz *et al.* 1992). The color aerial photography used in this project, which lacked either unique bands or an infrared channel, also primarily detected qualities of the vegetation canopy. Additionally, some of the signature training sets consisted of multiple dominant species. Thus, the findings of Treitz *et al.* (1992) can be considered in the context of the training methodology used in this project and highlight the importance of working with identification classes and subsequent training sites which are spectrally uniform, adequately representative of identification classes and correlated with the spectral data available in the image.

Identification classes and subsequent training sites used in this project were based on previously established vegetation sampling plots where micro-topographic association was initially determined on observable characteristics (using low altitude aerial photography and field observation) and further refined with TWINSPAN clustering based on detailed vegetation sampling. Because vegetation plots were originally selected for ecological field analysis, remote sensing and image processing were not considered. While classes developed by statistical routines such as TWINSPAN may be ecologically similar based on species abundance, composition and percent cover yet distinct based on the present or absence of indicator species, the resulting classes may not be spectrally similar nor adequately distinct. Thus, the compatibility of pre-determined, ground data based TWINSPAN-generated identification classes with the spectral qualities of the data is an issue related to training site quality and signature development.

Successful supervised classification is greatly dependent upon the analyst's knowledge of the site under consideration. Research conducted by Scholz *et al.* (1979) found that "...the

major variable affecting correct classification accuracy is not the classifier, but the training method used in generating the class statistics. The most important aspect of training is that all cover types in the scene must be adequately represented by sufficient number of samples in each spectral subclass" (as cited in Campbell 1987, 315). Uniformity or homogeneity within training sets is important to successful classification (Campbell 1987, 314).

In retrospect, the manner in which I dealt with the creation of signatures from training sites extracted from the vegetation plots may have been inadequate. Species composition is heterogeneous within and among mounds and intermounds. This adds another level of complexity to differentiating the two cover types, as community structure and composition vary from mound to mound and within the intermound regions. Such factors as differential effects of burning within the research space, environmental factors such as local micro-topography and soil characteristics, drainage patterns, proximity to alien seed sources, and several plots straddling the mound-intermound boundary generally increase class heterogeneity thus increasing the complexity of class signatures. The generalizing effect of the single, wide spectral data band magnified problems associated with intra-class complexity and together increased the chances of statistical similarity between signature sets further hindering signature distinction.

Variability was somewhat accounted for by dividing the research unit into treatment subspaces, training and classifying each separately. Treitz *et al.* (1992) suggest that one way TWINSPAN clusters might perform better with spectrally distinct remotely sensed data would be to modify the parameter space on which TWINSPAN operates forming spectrally distinct TWINSPAN clusters by combining spectrally non-distinct species. In this case, training classes were not spectrally distinct; therefore, rather than modifying TWINSPAN classes, further division of micro-topographic signatures into spectral sub-units would have been appropriate.

This is especially evident in the intermound signatures which exhibit large standard deviations and bimodality, most prominent in Spaces 1 and 2 (Figure 6).

While TWINSPAN does develop a dendrogram where classes can be considered at various levels of aggregation (Treitz *et al.* 1992, 69), the binary classification scheme used in this research project did not account for variation within specific plots or community types. Thus, labeling training sites in a binary fashion generalizes variation and results in signature classes that are not necessarily spectrally distinct. By developing signatures for each training site within a research space, signatures could be examined for outliers, anomalies, and compared to others within the same micro-topographic class. This would allow the editing of outliers within a training site and reveal vegetationally associated micro-topographical class anomalies, such as plot 9, to be developed as a spectrally distinct sub-classes. Through post-classification aggregation of micro-topographic sub-classes a binary thematic map could be developed.

Because of the generalizing effect of a single, wide data band and the associated loss of spectral information, I would suggest that the classification still be conducted on a space by space basis. The use of multiple, spectrally distinct data bands might enable the entire RNA to be treated as a single unit. Yet, due to treatment (fire) related differences in community makeup associated with the micro-topography, signature distinction based on binary micro-topographic labels, even with the use of sub-classes, may be difficult. In that case, the classification categories could focus on plant communities at a level of disaggregation finer than mound-intermound association.

I do not believe the aforementioned training alternatives to the classification method used in this paper would significantly increase classification accuracies in Space 3. Extreme similarity of signatures, comparatively low standard deviations and approximately normal

distributions leave little hope of creating spectrally distinct classes using the wide, 8-bit, monochromatic image available to this project. The possibility for enhanced signature distinction with the use of multiple data bands was most apparent in Space 3. The addition of signatures based on the Relative Richness pseudo-band did not appreciably affect overall classification accuracy. This may be due to (1) derivation of the pseudo-band from the original image, (2) inappropriate filter size (3x3 pixel) of the Relative Richness index for the textual pattern of the mound-intermound communities and/or (3) image acquisition not conducted during a period of maximum textural diversity between vegetation classes.

While the Relative Richness index had a smoothing effect, thus reducing the difference of means for Spaces 1,2 and 4, the inclusion of signatures extracted from this additional band helped distinguish micro-topographic classes within Space 3. Space 3 signatures from the single original band exhibited extremely close means and a larger standard deviation for intermounds yet, the signatures also exhibit large differences in range (109) and digital number diversity (22). By considering relative digital diversity within the moving filter, the index was able to create signatures with greater separation of means. The inclusion of the additional information provided by the Relative Richness index aided in class distinction for Space 3.

Choice of algorithm had minimal impact on overall classification accuracies. Maximum likelihood had a slightly higher overall accuracy rate at 71.68% than minimum distance at 68.83% (Table 4). Mounds tended to have higher accuracies with maximum likelihood. Intermound, on the other hand, classed better with the minimum distance algorithm. The minimum distance classifier, which does not consider variance nor covariance of signatures, tended to better class intermounds at the expense of mounds. Thus, while total area classed as mound was higher regardless of algorithm, the relative percentage of area classed as

mound was higher and intermound lower with the maximum likelihood classifier than the minimum distance classifier (Table 5). The limitation of minimum distance for dealing with variance and covariance of signatures is especially apparent in Space 3 where extremely close class means (difference of 0.41 for training plots and 0.13 for vegetation plots) and high intermound standard deviation (21.68) led to the majority of pixels being classed as intermound (94.75%) (Table 4).

Performance levels for the maximum likelihood classified image were better than those based on the minimum distance algorithm. Accuracies achieved using the maximum likelihood algorithm, with signatures based on the original band and then with the inclusion of the Relative Richness based signatures, were close enough to make selection for final output difficult. The greatest difference was in the percentage of pixels left as unclassified with the single band strategy leaving 4.17% of the accuracy assessment area unclassified while the two band strategy left 6.33% as unclassified. Total area per space left as unclassified was also higher using the combined signature set (Table 5). Comparison of the classified images to the original image revealed that in both cases the majority of unclassified pixels outside the vegetation plots were on the fringes of the RNA representing small stands of trees. Because both classification strategies identified the stand areas as unclassifiable, I decided that the strategy resulting in a lower percentage of unclassified pixels within the vegetation plots was desirable. Therefore, the output image resultant of the maximum likelihood classifier with signatures derived from the original image was selected for final cartographic output.

CONCLUSION

The objectives of this research project were to: (1) locate and map the boundaries of the RNA and research burn units, (2) locate and map the spatial distribution of permanent vegetation sampling plots within the RNA and (3) map the extent of the vegetationally associated mound-intermound micro-topographic pattern of the RNA using digital image processing and classification techniques. These objectives were met with varying degrees of success. The use of Trimble's GPS, IDRISI's low cost, PC compatible image processing/GIS software and a monochromatic image with values comprised of the visual spectrum proved sufficient to create an accurate digital spatial data base. The single band image and associated color palette was satisfactory for creating a visual and spatial data base but was lacking in the spectral information required for digital "spectral" classification.

To increase analytical abilities, thereby increasing both classification possibilities and accuracies, additional spectral information is desirable. An increase in the number of spectral bands, together with the restriction of band information to a narrow region of the electromagnetic spectrum, would provide information conducive to signature separability in spectral space. Thus, it is recommended that at the least, three bands comprising the red, green and blue components of the visual spectrum be used to increase signature distinction. Inclusion of an infrared channel is extremely desirable for distinguishing types of vegetation, vegetation condition as well as separating vegetation, soil and water. As an indicator of vegetation vigor, the inclusion of signatures based on infrared values might help in separating mound versus intermound classes during periods of differing growth status, thus placing less emphasis on either color or textural differentiation.

Because TWINSPAN developed classes are not necessarily spectrally distinct further emphasis needs to be placed on creating signatures that are spectrally unique. In addition to

the use of multiple data bands, spectrally distinct class categories could be developed in such ways as: (1) switching to a dominant species/vegetation based classification system, (2) modifying parameter space on which TWINSPAN operates by combining spectrally non-distinct species to form spectrally distinct clusters (Treitz *et al.* 1992, 80), or (3) modifying the training method by separating classes into spectrally distinct sub-classes. Because the TWINSPAN generated micro-topographically associated vegetation classification system is both firmly established and suitable to the RNA environment, I suggest that option number 3 be further investigated.

REFERENCES

Boag, Peter G. 1992. Environment and Experience. Berkeley: University of California Press.

Boyd, Robert. 1986. Strategies of Indian Burning in the Willamette Valley. *Canadian Journal of Anthropology*. 5:65-86.

Campbell, James B. 1987. Introduction to Remote Sensing. New York: Guilford Press.

Eastman, Ronald J. 1992. IDRISI Technical Reference and IDRISI User's Guide. Clark University, Graduate School of Geography. Worcester, Massachusetts. Version 4.0.

----ERDAS Field Guide. 1991. ERDAS Inc. Atlanta, GA. Second Edition, Version 7.5.

Franklin, Jerry F. 1972. Willamette Floodplain Research Natural Area. In Federal Research Natural Areas in Oregon and Washington--A Guidebook for Scientists and Educators. USDA, Forest Service and Range Experimental Station, Portland, Oregon.

Frenkel, Robert E. and Rosemary A. Streatfeild. 1994. Effects of Fire on Vegetation of the Willamette Floodplain Research Natural Area, W.L. Finley National Wildlife Refuge, 1991. Unpublished Report. Department of Geosciences, Oregon State University, Corvallis.

Frenkel, Robert E. and Rosemary A. Streatfeild. 1993. Restoring Willamette Valley Wet Prairie in Oregon with Fire. Unpublished paper presented at the 89th. Annual Meeting of the Association of American Geographers, Atlanta, Georgia.

Gunther, Erna. 1973. The Ethnobotany of Western Washington: the Knowledge of Indigenous Plants by Native Americans. Seattle: University of Washington Press.

Habeck, James. 1961. The Original Vegetation of the Willamette Valley, Oregon. *Northwest Science*. 35:65-77.

Hall, Roberta L., Robert Morrow and J. Henry Clarke. 1986. Dental Pathology of Prehistoric Residents of Oregon. *American Journal of Physical Anthropology*. 69:325-334.

Hurn, Jeff. 1989. GPS: A Guide to the Next Utility. Sunnyvale, California: Trimble Navigation.

Jackson, Philip L, and A. Jon Kimerling Editors. 1993. Atlas of the Pacific Northwest. Corvallis, Oregon: Oregon State University Press.

Johannessen, Carl., William A. Davenport, Artimus Millet and Steven McWilliams. 1971. The Vegetation of the Willamette Valley. *Annals of the Association of American Geographers*. 61:286-306.

Lillesand, Thomas M., and Ralph W. Kiefer. 1979. Remote Sensing and Image Interpretation. New York: Wiley.

Streatfeild-Welch, Rosemary A. 1995. Ecological Survey and Interpretation of the Willamette Floodplain Research Natural Area, W.L. Finley National Wildlife Refuge, Oregon. M.S. Thesis. Oregon State University, Corvallis.

Towle, Jerry C. 1979. Settlement and Subsistence in the Willamette Valley: Some Additional Considerations. *Northwest Anthropological Research Notes*. 13:12-21.

Treitz, Paul M., Philip J. Howarth, Roger C. Suffling and Paul Smith. 1992. Application of Detailed Ground Information to Vegetation Mapping with High Spatial Resolution Digital Imagery. *Remote Sensing of Environment*. 42:65-82.

Appendix 1. Indigenous uses of plant species found in the Willamette Floodplain Research Natural Area, W.L. Finley National Wildlife Refuge.

Achillea millefolium		medicine		
Camassia quamash	food			
Cirsium sp.		medicine		
Eriophyllum lanatum		medicine		
Fragaria sp.	food	medicine		
Galium aparine			charm	
Galium triflorum		medicine	charm	
Potentilla gracillis			charm	
Rhamnus purshiana	food	medicine		materials
Rosa spp.	food	medicine		
Rumex spp.	food	medicine		
Rumex acetosella	food	medicine		
Spiraea spp.		medicine		material
Symphoricarpos albus	food	medicine		
Vicia americana		medicine		

Source: List complied from those species listed in Gunther's Ethnobotany of Western Washington (1973) and identified as species present in the RNA according to Frenkel and Streatfeild's vegetation sampling records.

Appendix 2. Global Positioning System rover and Community Base-station parameter settings used in this research project.

Oregon State University Community Base-station

Location: 44 34' 5.664" N 123 16' 170" W

Ellipsoidal Elevation: 71.308 meters

Critical Setting:

- Position Interval: 0.05 seconds
- Filter Constant: 0.20
- PDOP Mask: 10
- PDOP Switch: 08
- Elevation Mask: 13
- Signal to Noise Ratio Mask: 0.07

Pathfinder Rover

Critical Settings:

- STS Mode on MASK Screen
- Position Interval: 001 seconds
- Filter Constant: 0.20
- Maximum PDOP: 06
- 2D Switch: 06
- Elevation Mask: 18
- Signal to Noise Ratio: 07

Informational Settings:

- SET UP Mode on Set Up Screen
- Dynamics Code: Land
- Position Fix Mode: (manual) 3D
- Altitude Reference: Mean Sea Level (MSL)
- North Reference: True North
- Units of Measurement: Meters
- Coordinate System: Universal Transverse Mercator
- Datum: WGS 84
- Time Zone: UTC

- SET UP Mode on Communications Screen
- Communications Protocol: XMODE
- Baud Rate, Parity, Data Bits, Stop Bit: 9600, N, 8, 1
- RTCM: non-differential GPS
- Stale RTCM: 0.001 seconds

USGS GPS Super-station (E141) NGS Survey

Location: UTM Northing: 4915366.440 UTM Easting: 476815.244

Elevation: 80.75 meters (264.3 feet)

Appendix 3. Global Positioning System rover display data recorded prior to and concluding each positional reading.

PLOT #	FILE #	PRE SAT.	POST SAT.	PRE PDPO	POST PDOP	PRE ACC.	POST ACC.	3-D	DURA-TION	SAMPLE SIZE
1	B101122B	7	7	2.6	2.5	100	100	Y	5.00	220
2	B021820A	6	5	2.9	3.5	300	100	Y	5.01	211
3	B101218C	5	6	3.4	3.6	300	300	Y	5.00	213
4	B101218A	6	5	2.9	3.3	100	300	Y	5.22	244
5	B101217B	6	6	2.9	2.9	100	100	Y	5.25	226
5A	B100123B	6	6	2.5	2.5	100	100	Y	5.00	214
6	B101221C	6	6	3.2	3.2	300	300	Y	5.55	248
7	B101221A	6	6	3.6	3.4	300	300	Y	5.00	242
8	B101219C	7	7	2.8	2.7	100	100	Y	5.00	216
9	B101219B	7	7	3.2	3.1	300	100	Y	5.00	215
10	B101122D	7	6	2.4	2.8	100	100	Y	5.00	218
11	B101120A	6	6	3.5	3.4	300	300	Y	5.00	187
12	B101119B	7	7	3.4	3.2	300	300	Y	5.34	209
13	B101119D	7	6	2.6	3.8	100	300	Y	5.16	234
14	B100722C	6	8	3.2	2.7	300	100	Y	5.08	215
15	B100722A	6	6	3.2	3.3	300	300	Y	5.00	214
16	B100721D	7	6	3.1	3.2	100	300	Y	5.00	219
18	B100722D	8	7	2.8	2.6	100	100	Y	5.00	226
18A	B100722B	6	6	3.2	3.2	300	300	Y	5.02	210
19	B100723B	6	6	2.4	2.5	100	100	Y	5.01	214
20	B021821A	5	7	3.1	2.6	100	300	Y	5.00	218
21	B100721A	6	6	3.0	3.1	100	100	Y	5.17	222
22	B100721D	7	6	3.1	3.2	100	300	Y	5.00	219
23	B100719D	7	7	3.2	3.0	300	100	Y	5.00	216
24	B100719C	6	7	3.9	3.5	300	300	Y	5.01	211
25	B100720A	7	6	2.6	3.8	100	300	Y	5.02	212
26	B100719B	7	7	3.1	3.3	100	300	Y	5.00	211
27	B100719A	6	7	3.7	2.9	300	100	Y	5.24	226
28	B100718D	6	6	3.6	3.7	300	300	Y	5.00	212
29	B100718B	6	6	2.9	2.9	100	100	Y	5.01	218
30	B100718A	6	6	3.0	2.9	100	100	Y	5.00	215
31	B100720B	6	****	3.4	****	300	****	Y	5.01	212
32	B100720C	6	8	3.2	2.3	300	100	Y	5.00	202
33	B100718C	5	5	3.3	3.4	300	300	Y	5.00	227
34	B100717A	5	5	3.5	3.3	300	300	Y	5.00	222
35	B100717B	5	6	3.2	3.0	300	100	Y	5.00	214
36	B100717C	7	7	3.0	2.9	100	100	Y	5.00	217

* PRE-POST SATELLITE = Number of satellites being tracked.
* PRE-POST PDOP = Percent dilution of precision.
* PRE-POST ACCURACY = Accuracy in meters.
* DURATION = Length of sample in minutes.
* SAMPLE SIZE = Number of samples positions.

Appendix 4. Differentially corrected GPS determined UTM locations of the northwest corner for the 38 permanent vegetation plots (+/- 2.54 meter accuracy).

Plot Number		Sample Size	Mean UTM (m)	Standard Deviation
1	Northing	220	4918838.39	1.95
	Easting	220	475716.03	1.58
2	Northing	211	4918768.87	3.30
	Easting	211	475662.44	2.68
3	Northing	213	4918605.20	2.59
	Easting	213	475700.99	2.06
4	Northing	243	4918635.82	1.98
	Easting	243	475757.47	2.05
5	Northing	226	4918646.83	2.03
	Easting	226	475775.14	2.26
5A	Northing	214	4918643.49	1.60
	Easting	214	475826.83	1.97
6	Northing	248	4918617.27	2.97
	Easting	248	475863.72	1.77
7	Northing	242	4918545.80	1.60
	Easting	242	4757908.02	1.52
8	Northing	217	4918380.95	2.56
	Easting	217	475864.07	1.61
9	Northing	**	4918378.24	4.17
	Easting	**	475793.03	2.41
10	Northing	202	4918761.35	2.14
	Easting	202	475793.00	1.77
11	Northing	188	4918192.40	3.94
	Easting	188	476557.22	3.15
12	Northing	209	4918182.95	3.48
	Easting	209	476503.06	2.00
13	Northing	235	4918232.73	2.81
	Easting	235	476469.13	2.75
14	Northing	216	4918016.41	3.34
	Easting	216	476472.65	2.86
15	Northing	214	4917865.57	1.72
	Easting	214	476336.35	2.81
16	Northing	219	4917856.60	1.87
	Easting	219	476395.76	2.92

Appendix 4 (Continued)

Plot Number		Sample Size	Mean UTM (m)	Standard Deviation
17	Northing	232	4918109.27	2.71
	Easting	232	476320.36	2.81
18	Northing	226	4917954.86	2.01
	Easting	226	476485.01	2.43
18A	Northing	209	4918013.37	4.16
	Easting	209	476376.06	2.94
19	Northing	214	4918124.61	1.61
	Easting	214	476498.97	3.45
20	Northing	218	4918005.70	2.80
	Easting	218	476522.77	2.91
21	Northing	222	4917649.59	2.71
	Easting	222	476487.99	2.55
22	Northing	215	4917568.42	2.21
	Easting	215	476485.86	1.73
23	Northing	216	4917427.73	3.18
	Easting	216	476319.38	2.31
24	Northing	204	4917400.69	3.81
	Easting	204	476405.85	1.85
25	Northing	212	4917395.02	2.52
	Easting	212	476508.55	1.78
26	Northing	212	4917272.64	3.07
	Easting	212	476389.94	2.37
27	Northing	226	4917228.36	2.22
	Easting	226	476408.12	2.10
28	Northing	212	4917170.37	3.03
	Easting	212	476445.69	1.26
29	Northing	219	4917083.09	2.67
	Easting	219	476399.47	2.21
30	Northing	216	4916863.16	1.95
	Easting	216	476451.78	2.27
31	Northing	212	4917216.29	1.70
	Easting	212	476646.20	1.49
32	Northing	202	4917181.53	1.57
	Easting	202	476592.68	2.28
33	Northing	227	4917065.20	1.54
	Easting	227	476527.38	1.87

Appendix 4 (Continued)

Plot Number		Sample Size	Mean UTM (m)	Standard Deviation
34	Northing	223	4916961.64	1.38
	Easting	223	476604.04	1.41
35	Northing	214	4916834.73	2.05
	Easting	214	476618.72	2.04
36	Northing	217	4916864.91	1.60
	Easting	217	476525.53	2.55

Note: The location of plot 9 was visually determined using the rectified digital image.

Appendix 5. Differentially corrected GPS determined UTM locations of the northwest corner for the six 1983 research plots (+/- 2.54 meter accuracy).

Plot Number		Sample Size	Mean UTM (m)	Standard Deviation
1	Northing	236	4918935.17	2.19
	Easting	236	475703.66	2.94
2	Northing	248	4918664.04	4.18
	Easting	248	475723.31	2.31
3	Northing	197	4918462.49	2.62
	Easting	197	475759.18	2.28
4	Northing	192	4918252.10	3.36
	Easting	192	475961.94	2.55
5	Northing	215	4918106.18	1.44
	Easting	215	476272.16	2.13
6	Northing	234	4918250.23	3.21
	Easting	234	476503.70	1.47

Appendix 6. Positional Readings of USGS Superstation (E111)

Date		Sample Size	Mean UTM	Standard Deviation	Minimum UTM	Maximum UTM
10/7/93	Northing	215	4915368.98	2.32	4915363.44	4915374.47
	Easting	215	476816.76	1.55	476811.92	476820.13
10/11/93	Northing	237	4915365.16	2.36	4915358.78	4915371.12
	Easting	237	476815.23	2.26	476810.17	476821.18
10/12/93	Northing	242	4915366.15	1.57	4915362.01	4915370.23
	Easting	242	476815.45	2.47	476808.07	476820.29
10/14/93	Northing	205	4915368.19	2.88	4915360.61	4915374.16
	Easting	205	476817.21	1.59	476813.65	476820.31

Results of the pre field data collection GPS tests are recorded in Universal Transverse Mercator units.

USGS Recorded Superstation (E141) Location: UTM Northing: 4915366.440

UTM Easting: 476815.244